Available online at www.CivileJournal.org

Civil Engineering Journal

(E-ISSN: 2476-3055; ISSN: 2676-6957)

Vol. 11, No. 06, June, 2025

Circularized and Corner-Rounded Rectangular Reinforced Concrete Columns Wrapped with CFRP Under Eccentric Compression

Tung D. Dang [1, 2], Canh Tuan Nguyen [1, 2], Vui Van Cao [1, 2*]

[1] *Faculty of Civil Engineering, Ho Chi Minh City University of Technology (HCMUT), District 10, Ho Chi Minh City, Vietnam.*

[2] *Vietnam National University Ho Chi Minh City, Linh Trung Ward, Thu Duc City, Ho Chi Minh City, Vietnam.*

Received 13 March 2025; Revised 23 May 2025; Accepted 27 May 2025; Published 01 June 2025

Abstract

This paper presents experimental and analytical investigations on the behavior and mechanical properties of carbon fiber reinforced polymer (CFRP) confined circularized and corner-rounded rectangular reinforced concrete (RC) columns under eccentric loading. Twelve RC columns with cross sections of 150×200 mm were tested. Two columns were used as control specimens. Five columns were circularized and then wrapped with five CFRP configurations. The other five columns were corner-rounded and then wrapped with the above configurations. These twelve columns were eccentrically loaded until they failed. The results indicated that CFRP-confined circularized RC columns failed by CFRP rupture at the eccentric side, while CFRP-confined corner-rounded RC columns failed by CFRP rupture localized at corners. The outstanding effectiveness of the circularization method was its increase in the ultimate load of CFRP-confined circularized RC columns by 3.0–4.3 times that of the control columns. In contrast, the corner-rounding method moderately increased the ultimate load of CFRP-confined corner-rounded RC columns by 1.3–1.7 times that of the control columns. The circularization method outstandingly improved the elastic stiffness by 273.9%–419.3% compared with that of control columns, whereas the corner-rounding method exhibited no effect on the elastic stiffness. The rotation ductility of CFRP-confined circularized and corner-rounded RC columns significantly improved to high ductility when confined with more than 1.33 CFRP layers. Theoretical analyses were performed, and simple models were proposed for reasonably estimating the ultimate loads of the CFRP-confined circularized and corner-rounded RC columns under eccentric loading.

Keywords: Circularization; Corner-Rounding; CFRP Confinement; Eccentric Compression; Reinforced Concrete; Column.

1. Introduction

With the development of society, civil engineering structures are facing a higher load demand. For example, heavier trucks acting on bridges or higher loads on building structures due to changes in use. In such circumstances, the load-carrying capacity of columns and beams has to be upgraded. One of the upgrading methods is to use fiber-reinforced polymer (FRP) because of its advanced mechanical properties. Its flexible applications offer advantages in upgrading structures by improving the flexural strength [1-3], shear strength [4-7], compressive strength [8-10], or combined strengths [11, 12]. The flexible applications of FRP also offer several repairing methods for concrete [13-15], RC beams/columns [16-20], beam-column joints [21], and RC frames [22-24].

One of the most common applications of FRP is to wrap concrete or RC columns to provide the confinement effect. The effectiveness of FRP confinement has been widely proven in the literature. The strength and ductility of concrete confined by FRP improved substantially [25-29]. FRP wrapping has been confirmed as an appropriate solution for

* Corresponding author: cvvui@hcmut.edu.vn

http://dx.doi.org/10.28991/CEJ-2025-011-06-022

externally confining RC structures that are poorly confined by the deficient internal stirrups [8, 30] due to its uniform/distributed confinement. External FRP wrapping can confine the whole sections of members, whereas internal stirrups confine only the concrete core surrounded by the stirrups. Furthermore, the internal confinement by steel stirrups is significantly weaker than that by the external FRP wrapping. Thus, FRP confinement surpasses steel stirrup confinement in absorbed energy capacity [31, 32] and strength and ductility [32, 33].

Stress concentration is an issue of FRP confinement applied to square or rectangular columns. Stress concentration at corners leads to earlier rupture of FRP, while column sections still exist unconfined areas, namely ineffective regions. One of the simple methods to mitigate these issues is that corners of rectangular/square columns are rounded. Consequently, the effectiveness of FRP confinement is improved [34-36]. However, the corner-rounding method encounters the limited radius. The existing internal transverse and longitudinal steel does not allow for a large rounding radius. The issues of stress concentration, ineffective area, and early rupture of FRP are still pending in the corner-rounding method. Another method to mitigate the above-mentioned issues is the curvilinearization method, which has been conducted by researchers such as Zhu et al. [37] and Zeng et al. [38]. The performance of FRP-confined shape-modified columns was reviewed by He & Zeng [39]. A method that combines the shape modification, expansive concrete, and FRP confinement has been used by researchers, such as Chris & Zihan [40, 41] and Yan and Pantelides [42]. They confirmed several advantages of this combined method.

Circularization is considered to be the strongest solution for eliminating the issues of stress concentration, ineffective area, and early rupture of FRP. This is attributed to the more uniform confining stress in circular columns than that in rectangular or square columns. The circularization technique has been investigated by researchers. Pham et al. [43] circularized RC columns wrapped these circularized columns with FRP and loaded until failure. The results indicated that circularized concrete and original concrete formed a composite material. The ductility of FRP-confined circularized columns substantially improved. Hadi et al. [44] found that stress concentration in CFRP-confined circularized columns was significantly reduced. The confinement effectiveness, load-carrying capacity, and ductility improved, confirming the effectiveness of the circularization method. Zeng et al. [45] also confirmed the effectiveness of the circularization method before FRP wrapping. The combination of circularization and partly FRP wrapping demonstrated a promising solution due to its economical and technical aspects. Hadi et al. [46] experimentally found that the circularization enhanced the load-carrying capacity and ductility of circularized square hollow RC columns. Jameel et al. [47] experimentally concluded that circularization reduced the stress concentration at corners and improved the strength and ductility of FRP-confined circularized hollow RC columns under axial compression. Mai et al. [48] experimentally found that the combination of circularization and partly CFRP wrapping enhanced the ductility and strength of square RC columns. Al-Tameemi & Akın [49] circularized square concrete columns by attaching precast concrete pieces to four sides of the columns and then wrapped these circularized columns with one GFRP layer. They confirmed that the retrofitting technique significantly improved the axial strength and deformation capacity of the columns.

Sectional circularization is widely known as the most effective method of shape modifications. This is attributed to the obvious uniform stress in FRP due to the circular/smooth surface. Therefore, the load-carrying capacity of concrete columns is substantially increased, being suitable for upgrading structures. The drawback of this method is that it adds load, which is the self-weight of circularized concrete, to structures. This drawback discourages structural engineers from selecting the circularization for their design solution. Additionally, the number of studies on FRP-confined circularized concrete columns seems to be limitedly found in the literature. Lastly, studies on the behavior of CFRP-confined circularized concrete columns under eccentric loading are seldom found in the literature. Therefore, it is necessary to clarify several technical aspects of FRP-confined circularized RC columns under eccentric loading, which is aimed at by this study.

Toward the above-mentioned aim, twelve RC columns were fabricated for testing (Section 2). Two columns were used as control columns. Five columns were circularized, while five columns were rounded at the corners. After circularizing or corner-rounding, five CFRP wrapping configurations were applied to these columns. These twelve columns were eccentrically loaded until they failed. The behavior and mechanical properties of the tested columns were analyzed and compared in Section 3. Theoretical analyses were performed, and simple models were proposed for estimating the ultimate loads of the CFRP-confined circularized and corner-rounded RC columns under eccentric loading, as presented in Section 4. Conclusions are drawn and presented in Section 5. Although the circularization method is accompanied by the additional self-weight, its effectiveness surpasses this issue and is superior to the corner-rounding method. The experimental and analytical results of this study provide technical information, improving confidence for structural engineers in selecting the circularization method for upgrading RC columns.

2. Experimental Program

2.1. Materials and Columns

Table 1 shows compositions of concrete used for casting specimens. Figure 1 shows the grading curves of stone and sand aggregates with the upper and lower bounds based on TCVN 7570:2006 [50]. The average compressive strength

of six standard cylinder samples at the age of 28 days was 28.083 MPa. Steel CB3 ϕ14 and ϕ6 were used for the longitudinal and transverse reinforcement, respectively. The average yield and ultimate strengths of five CB3 ϕ14 steel samples were 341.2 MPa and 419.1 MPa, respectively. The average yield and ultimate strengths of five steel ϕ6 samples were 332.7 MPa and 461.4 MPa, respectively. CFRP had a thickness of 0.167 mm/layer and an elastic modulus of 230 GPa, as provided by the manufacturer. The average tensile strength of five CFRP specimens was 3774.75 MPa.

Table 1. Concrete mix

No.	Material	Mass (kg)
1	Cement PC40	390
3	Stone 1 × 2 cm	1162
4	Sand	722
5	Water	147

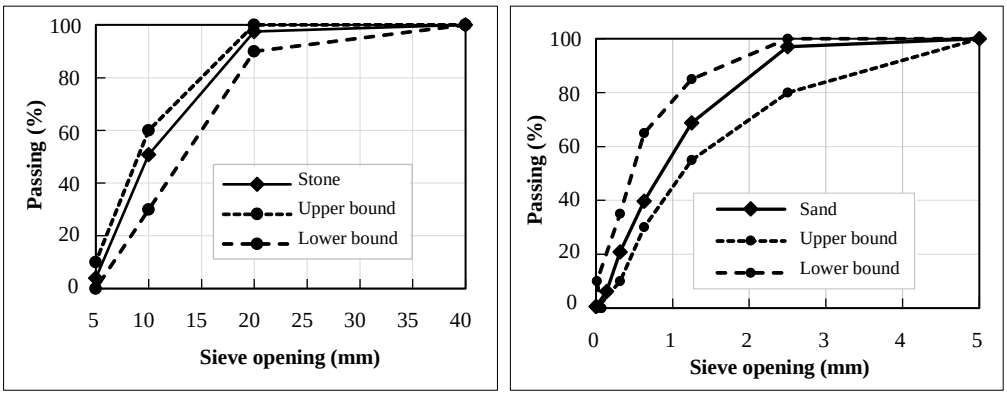

a) Coarse aggregate b) Fine aggregate

Figure 1. Grading curves of aggregates

Twelve RC columns divided into six groups, namely F0–F5, are presented in Table 2. Column labels are presented the third column of Table 2. The first two letters of column labels are "Co", "Ci", and "Ro", which are abbreviations of "Control", "Circularized", and "corner-Rounded", respectively. Group F0 includes two similar columns, Co-01 and Co-02, which were not retrofitted. These two columns, instead of one, were used as a control group to improve the accuracy. The last two letters of circularized and corner-rounded columns are F1–F5, in which F denotes CFRP and 1–5 represent five CFRP retrofitting configurations. In each of groups F1–F5, one column was circularized while the other column was rounded at corners. A similar CFRP retrofitting configuration was applied to the two columns of each group.

Table 2. Tested columns

No.	Group	Column	Shape modification	CFRP layer
1	F0	Co-01	Control	0
2		Co-02	Control	0
3	F1	Ci-F1	Circularized	0.33
4		Ro-F1	Corner-rounded	0.33
5	F2	Ci-F2	Circularized	1.00
6		Ro-F2	Corner-rounded	1.00
7	F3	Ci-F3	Circularized	1.33
8		Ro-F3	Corner-rounded	1.33
9	F4	Ci-F4	Circularized	1.67
10		Ro-F4	Corner-rounded	1.67
11	F5	Ci-F5	Circularized	2.00
12		Ro-F5	Corner-rounded	2.00

Figure 2-a shows the original RC columns with dimensions of 150 × 200 × 500 mm. 4ϕ14 bars were used for longitudinal reinforcement, and steel ϕ6 was used for the transverse reinforcement Figure 2-a). The concrete cover thickness was 25 mm measured to the center of the transverse reinforcement. Corner-rounded columns were rounded at corners with a radius of 20 mm, as shown in Figure 2-b. Columns with "Ci" in their labels were circularized with a diameter of 267 mm (Figure 2-c).

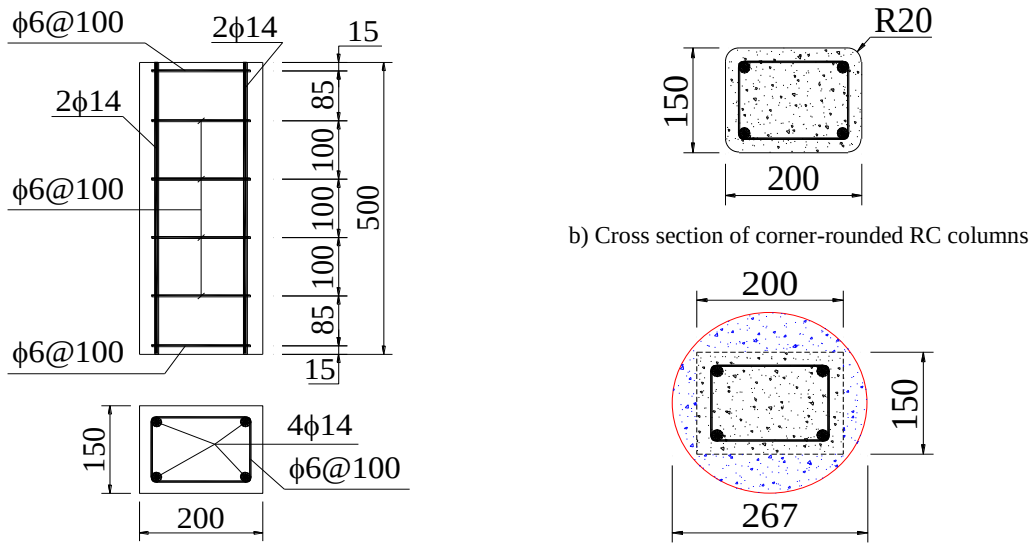

a) Original RC columns

b) Cross section of corner-rounded RC columns

c) Cross section of circularized RC columns

Figure 2. Original, corner-rounded, and circularized RC columns

Five configurations F1–F5 of CFRP retrofits are shown in Table 2, and their details are drawn in Figure 3. Columns Ci-F1 and Ro-F1 were wrapped by 33-mm CFRP strips with a clear distance of 84 mm, as shown in Figure 3-a. Columns Ci-F2 and Ro-F2 were wrapped by a full layer of CFRP, as shown in Figure 3-c. Columns Ci-F3 and Ro-F3 were wrapped by 33-mm CFRP strips (Figure 3-a) for the inner layer and a full layer (Figure 3-c) for the outer layer. Columns Ci-F4 and Ro-F4 were wrapped by 67-mm CFRP strips (Figure 3-b) for the inner layer and a full layer (Figure 3-c) for the outer layer. The overlap length was 100 mm. After CFRP wrapping as designed, 50-mm CFRP strips were applied to the top and bottom ends of the columns to avoid local damage at these locations due to stress concentration.

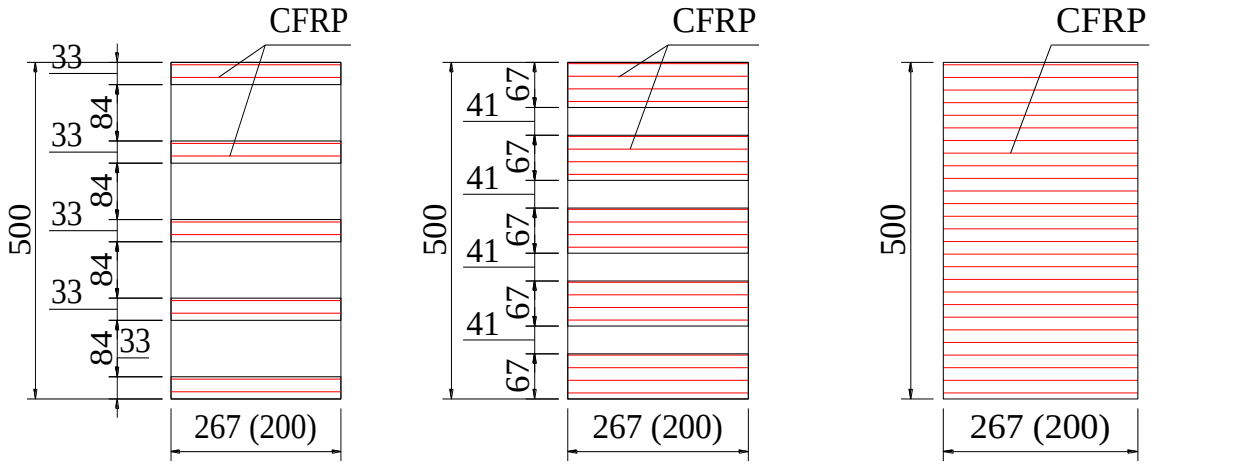

a) F1 and inner layer of F3

b) Inner layer of F4

c) F2, inner layer of F5, and outer layer of F4 and F5

Figure 3. CFRP retrofitting configurations for the tested columns (unit: mm)

Figure 4a shows five RC columns in the plastic formwork to be ready for circularization. During the casting of circularized concrete, concrete was directly compacted using a steel ϕ16 rod and was indirectly compacted using a vibration compactor on the outer surfaces of plastic formwork. Figure 4b shows twelve RC columns, which include two control RC columns at the far end, five circularized RC columns on the left row, and five RC columns on the right row. At 28 days after casting concrete, the plastic formwork was removed. Corners of five RC columns on the right row were rounded with a radius of 20 mm using a grinding machine. Figure 4c shows an example of CFRP wrapping for the circularized column Ci-F4, at which the outer layer of CFRP was being applied. Figure 4d shows these twelve columns after CFRP wrapping. Figure 4e shows these columns after grinding the top and bottom surfaces for being perpendicular to the column axes, to be ready for loading tests. Figure 4e illustrates the preparation steps of the columns.

a) Formwork for circularizing

b) After circularizing

c) CFRP wrapping in progress

d) After CFRP wrapping

e) Specimens before testing

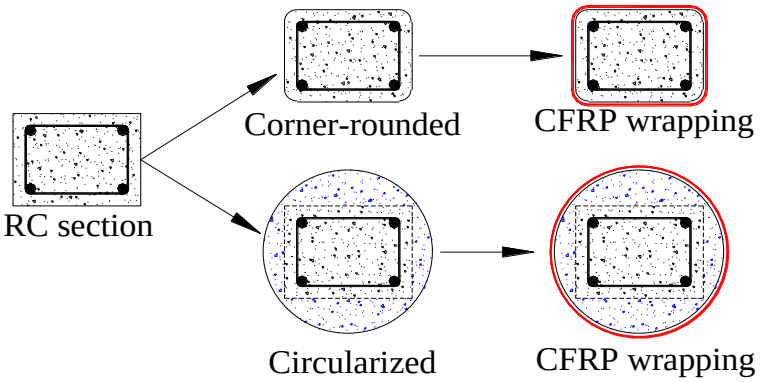

f) Illustration of the preparation steps

Figure 4. Preparation of the columns

2.2. Test Setup

Figure 5a is a photo of the real experimental setup. Its diagram is presented in Figure 5b. The instrument included three linear variable displacement transducers (LVDTs), a load cell, a hydraulic jack, a system to measure the axial displacements at two extreme sides of the tested columns, a system to measure the lateral expansion at the mid-height section of the columns, four thick steel plates, and two hemisphere steel bars welded to the top and bottom steel plates to create the eccentric loading. These two hemisphere steel bars were used to transfer the load on the eccentric line, which is parallel to the stronger principal axis of the cross sections. In other words, the eccentric line was perpendicular to the 200-mm side of the original RC cross sections.

LVDT 1 was used to measure the lateral expansion of the mid-height section. Because of the difficulty in installation and measurement at the surface of the columns, a system that includes a circular ring, an X-steel bar system, and a spring was used to transfer the displacement away from the columns' surface for being easier to install the LVDT. More importantly, damage to this LVDT caused by the failure of columns can be avoided. The displacements obtained from LVDT 1 are the elongations of the circumference of the column sections, which are used to calculate the lateral strain of the columns. Figures 5c and 5d show the LVDT 1 installed on the X-steel rod system to measure the displacement for calculating the lateral strain.

To eliminate the displacements due to contacts, the length for measurement of axial displacement was selected to be 400 mm at the middle of columns. Two steel rings were installed at 200 mm above and below the mid-height of the columns. LVDTs 2 and 3 were installed on these steel rings with a distance of 210 mm to the central axis for corner-rounded columns and circularized columns. These two LVDTs were symmetric with respect to the central axis of the column. After installation of columns and tools, the columns were loaded until they failed, while the loads and displacements were simultaneously recorded.

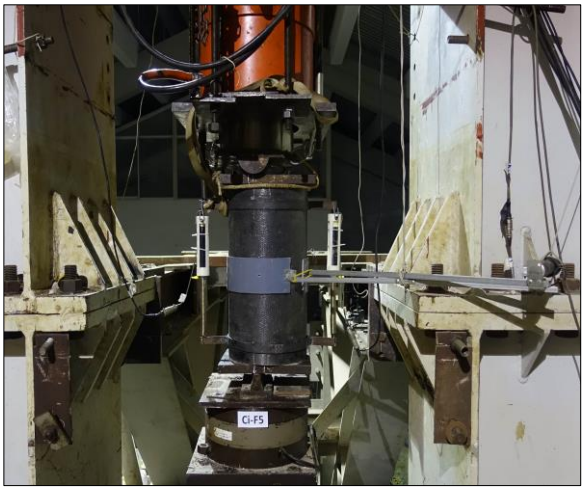

a) Real experiment setup

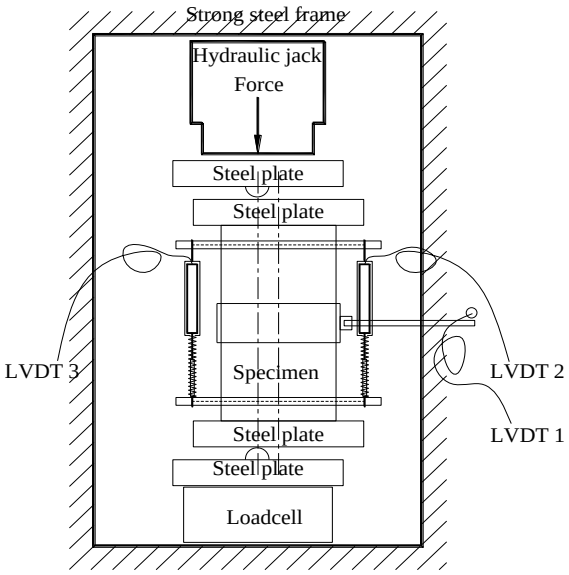

b) Diagram of the experimental setup

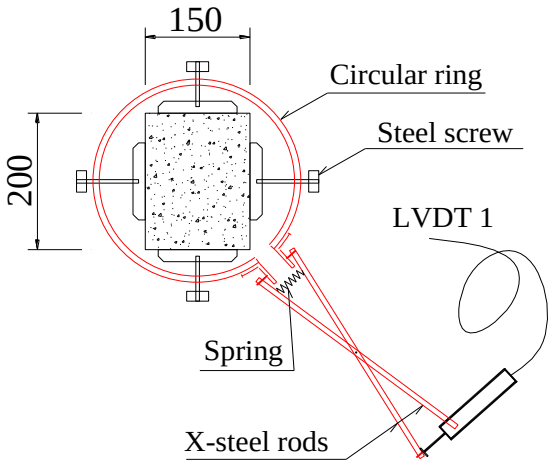

c) Measurement of the lateral expansion at the mid-height section of control and corner-rounded columns

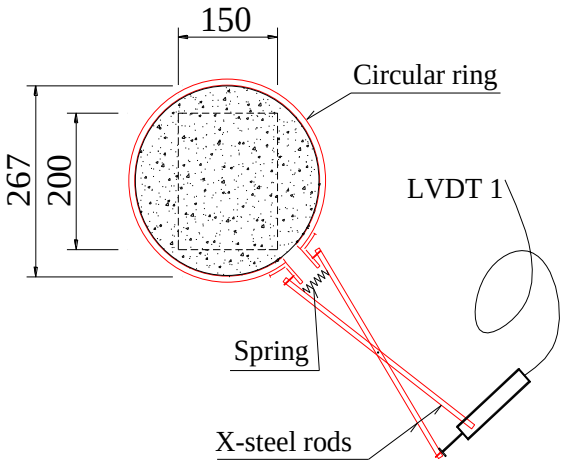

d) Measurement of the lateral expansion at the mid-height section of circularized columns

Figure 5. Experiment setup

3. Experimental Results and Discussions

3.1. Failure Patterns

The failure of the tested columns initiated and finalized at the extreme fibers of the eccentric side because of the highest compressive stress. In contrast, no failure initiated at the opposite side where the compressive stress was the lowest. Figure 6-a shows the failure patterns of the CFRP-confined circularized columns and control column Co-01. Figure 6-b shows the failure patterns of CFRP-confined corner-rounded columns and control column Co-02. Figure 6-c shows the side view of the failure patterns of all columns. For control columns Co-01 and Co-02, concrete in the compression extreme fiber crushed and propagated to a larger area when the load further increased. When displacement went beyond the ultimate point, a portion of concrete at corners spalled off. In contrast, no crack or crushing of concrete was observed on the other side of these control columns. This is due to the fact that the

eccentricity of the compression load was only ¼ of the dimension of the columns. This eccentricity is considered to be low and mainly caused compression to the column section. The crushing of concrete and the yielding of steel resulted in a descending load–strain branch.

a) CFRP-confined circularized columns Ci-F5–Ci-F1 and control column Co-01

b) CFRP-confined corner-rounded columns Ro-F5–Ro-F1 and control column Co-02

c) Side view of all tested columns

Figure 6. Failure modes

Moving on to the columns with configuration F1, the failure initiated at the extreme fibers of the eccentric side of the unwrapped CFRP sections. Increasing the load expanded the crushing region of concrete, creating the local stress on the edge of the CFRP strip nearby. For column Ci-F1, the local stress caused local damage of CFRP, which progressively developed to rupture of that CFRP strip. Then, CFRP splitting propagated toward the two sides and stopped at the middle. The rupture of the CFRP strip in column Ci-F1 resulted in a sharp drop in load. A tiny explosive sound due to the rupture of the CFRP strip was heard. For column Ro-F1, the crushing of concrete at the unwrapped section sufficiently decreased the load, whereas CFRP rupture did not occur.

For columns with the retrofitting configurations F2–F5, the failure modes are almost similar by rupture of CFRP, followed by crushing of concrete at the location of CFRP rupture. The failure initiated at the compressive eccentric side and then expanded to half of the specimens, whereas the other side of the eccentric loading experienced minor or no damage. This higher compressive stress acting on concrete resulted in higher lateral stress acting on CFRP. The local

damage of concrete initiated on extreme fibers of the highest stress at the eccentric side. Consequently, the local damage of concrete leads to local stress acting on CFRP, initiating the rupture of CFRP at that location. The rupture failure of CFRP quickly released the high confinement stress to zero stress, detaching the ruptured CFRP from concrete. CFRP detaching quickly expanded to ½ to 2/3 the circumference. An explosive sound was heard when CFRP was ruptured. Within a similar CFRP configuration, the level of the explosive sound of CFRP-confined circularized columns was stronger than that of corner-rounded columns. This is due to the fact that circularized columns have higher ultimate loads due to the more uniform stress in CFRP and the larger cross-sectional area of concrete; therefore, a higher amount of energy was released when CFRP was ruptured. Within a circularized or corner-rounded group, the explosive sound became stronger when going from the configuration F2 to F5. Importantly, there was no detaching/splitting of circularized concrete and original concrete in any circularized columns. This can be evidence that the circularized concrete and original concrete can work in a similar manner and can be considered as monolithic concrete. This observation can be a hypothesis for the analysis in Section 5.

Overall, the failure of columns retrofitted with CFRP configuration F1 and that of control columns were governed by the crushing of concrete. In contrast, the failure of columns retrofitted with CFRP configuration F2–F5 was governed by the rupture of CFRP with explosive sound. This is attributed to the release of high energy at the rupture of CFRP when the columns suddenly changed from the state of high confinement to the state of un-confinement. The explosive sound of CFRP-confined circularized columns was substantially stronger than that of CFRP-confined corner-rounded columns. This is attributed to the rupture of CFRP at higher and more uniform confinement and higher ultimate load of CFRP-confined circularized columns compared with those of CFRP-confined corner-rounded columns.

3.2. Load–rotation Curves

Figure 7-a shows a column with installed tools before loading. The length of columns for measuring the axial deformation was 400 mm. LVDTs 2 and 3 were installed symmetrically about the axial axis of the columns. The distance between these two LVDTs was L_{23} = 420 mm. Figure 7-b illustrates the deformation of deformed columns. During the tests, LVDT 2 elongated while LVDT 3 shortened. This observation should be taken into account when calculating the rotations and axial strains of the tested columns.

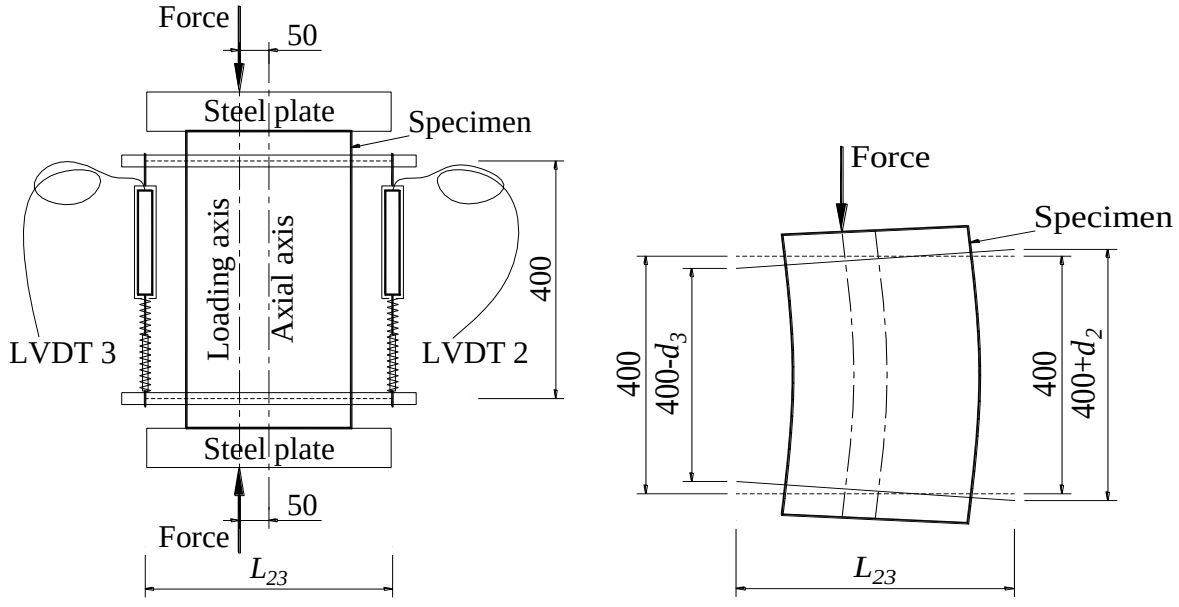

a) Before deformation b) During deformation

Figure 7. Deformation of the tested columns

Rotation is computed based on Equation 1, in which d_2 and d_3 are the displacements obtained from the two LVDTs 2 and 3, and L_{23} = 420 mm is the lateral distance between LVDTs 2 and 3. The load–rotation relationships are plotted in Figure 8. The coordinates of the yield and ultimate points are also shown in this figure. The yield rotations and the ultimate rotations were analyzed and compared in the later sections.

$$\theta = \frac{[(400+d_3)-400]-[(400-d_2)-400]}{L_{12}} = \frac{d_2+d_3}{L_{12}} \quad (1)$$

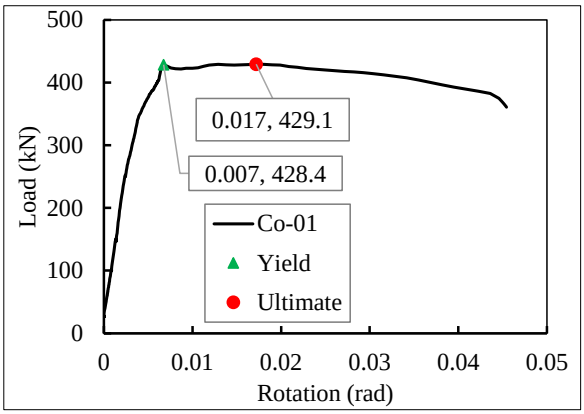

a) Co-01

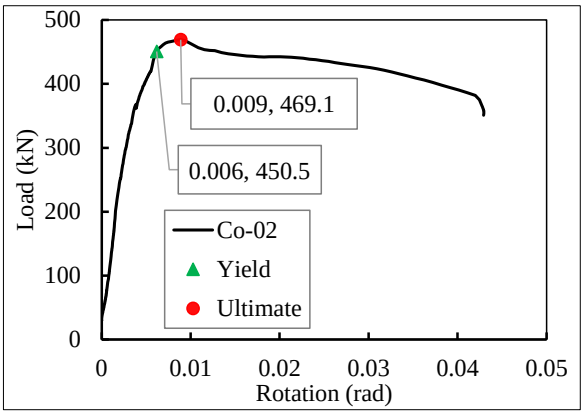

b) Co-02

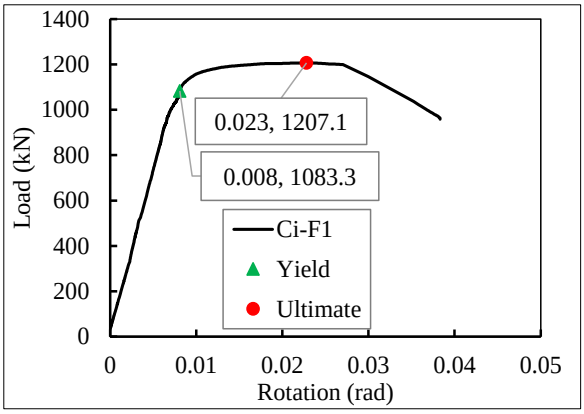

c) Ci-F1

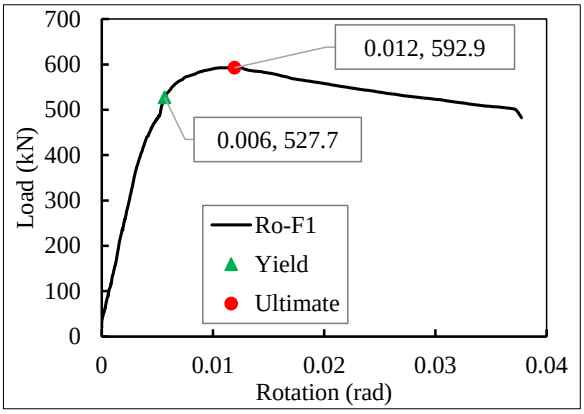

d) Ro-F1

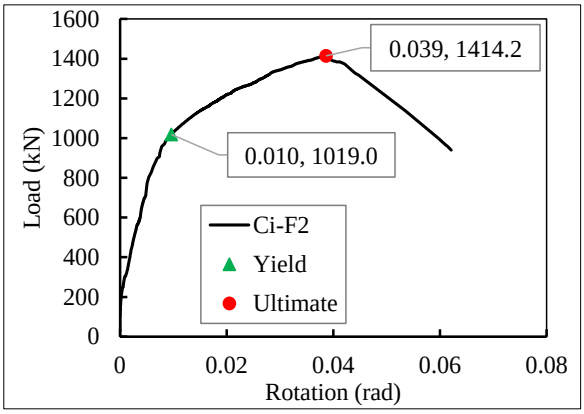

e) Ci-F2

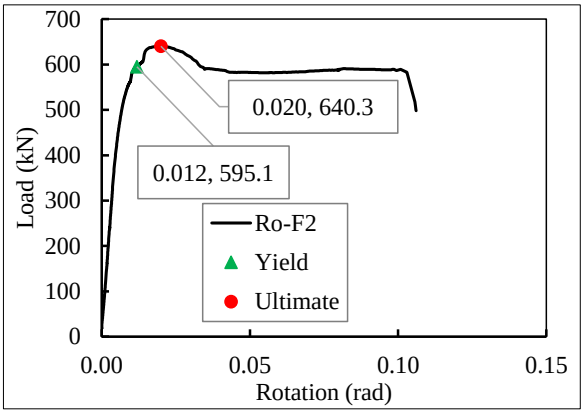

f) Ro-F2

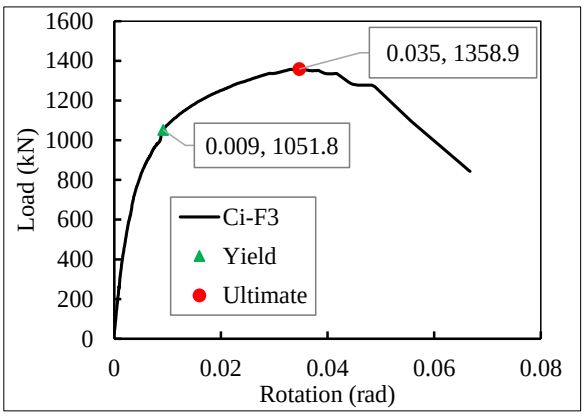

g) Ci-F3

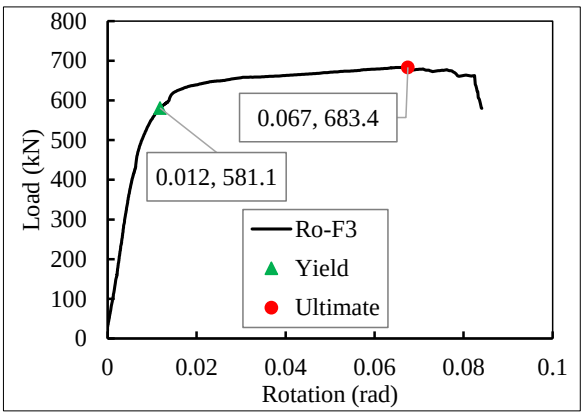

h) Ro-F3

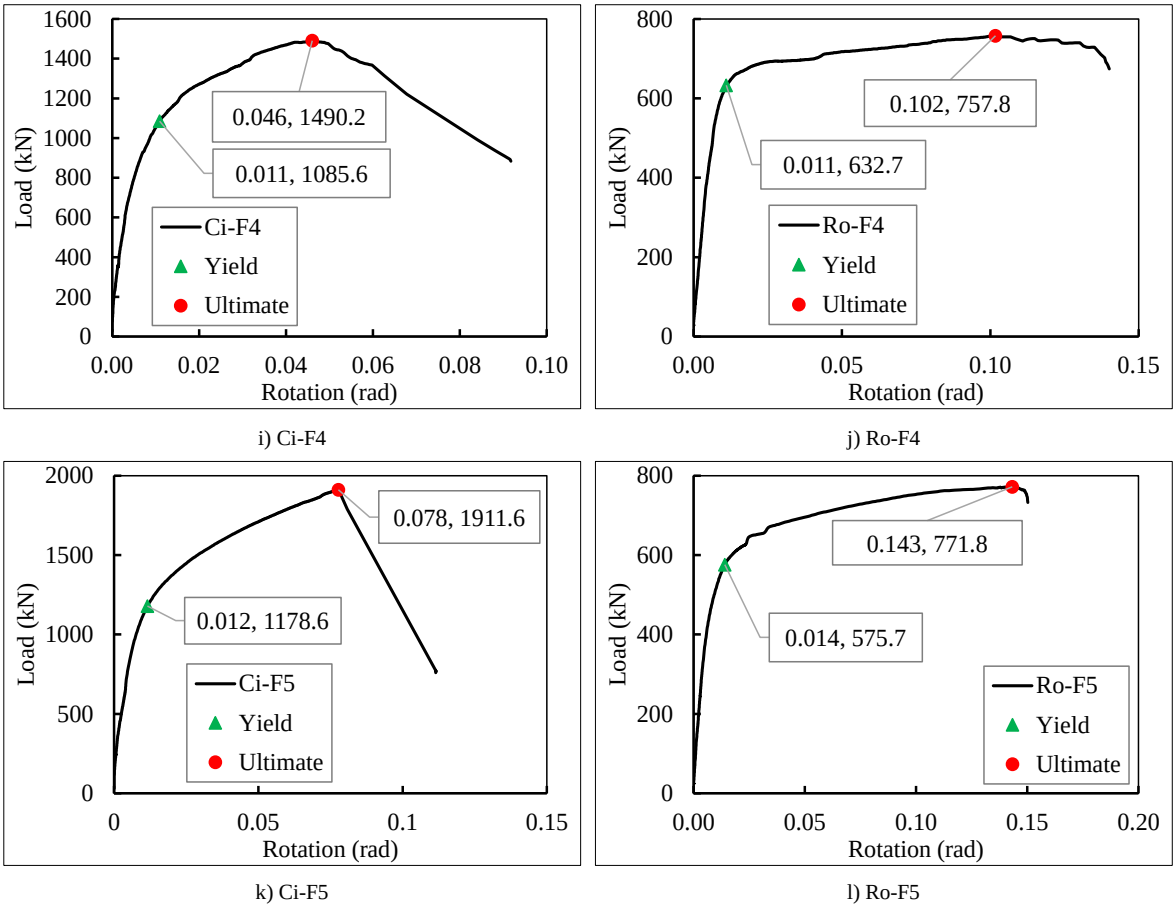

i) Ci-F4 j) Ro-F4

k) Ci-F5 l) Ro-F5

Figure 8. Load–rotation curves

For general comparison, these rotation–load curves are plotted in the same coordinate system, as shown in Figure 9. It can be seen in this figure that the curves can be classified into three groups: control group, corner-rounded group, and circularized group. It is clear that the curves of the control group are the lowest. With the corner-rounded technique and CFRP wrapping, the curves of corner-rounded group columns increased the elastic stiffness, slightly elongated the elastic branch, and significantly elongated the plastic branch. For the circularized group, the circularized technique and CFRP wrapping significantly increased the yield and ultimate strengths and increased the elastic and plastic stiffness, while the yield and ultimate rotations depended on CFRP retrofitting configurations. Detailed comparisons of the rotations are represented in the later section.

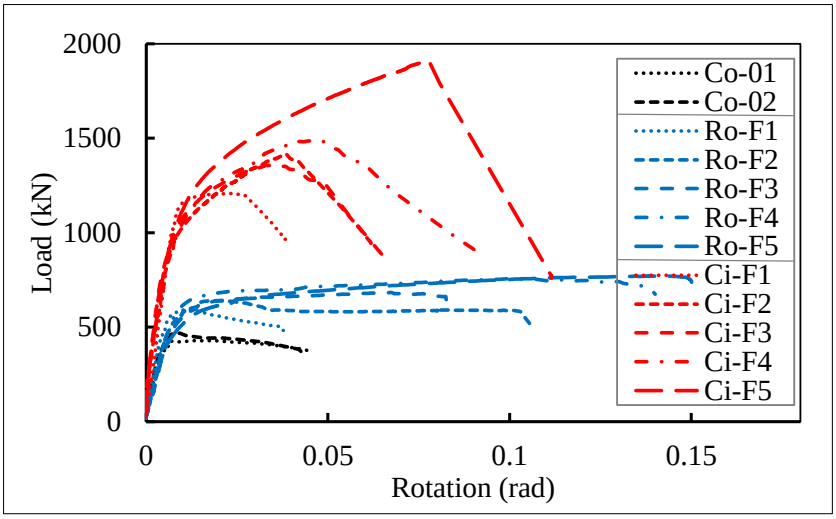

Figure 9. Comparison of load–rotation curves

3.3. Axial Load–Strain Curves

With reference to Figure 7, the axial strains were calculated by Equation 2, in which d_2 and d_3 are the axial displacements obtained from LVDTs 2 and 3, respectively, and L = 400 mm is the length of the column for displacement

measurement. The lateral strain was calculated by Equation 3, in which d_1 is the displacement obtained from LVDT 1, and C is the circumference of the tested columns. $C = 3.14 \times 267 = 838.38$ mm for the circularized columns, and $C = 2 \times (150 + 200) = 700$ mm for the corner-rounded and control columns.

$$\varepsilon_a = \frac{1}{L}\left[L - \frac{(L-d_3)+(L+d_2)}{2}\right] = \frac{d_3-d_2}{2L} = \frac{d_3-d_2}{800} \quad (2)$$

$$\varepsilon_l = \frac{d_1}{C} \quad (3)$$

Figure 10 shows the axial load–axial strain curves and the axial load–lateral strain curves of the tested columns. Due to the significant variations of axial loads, adaptive coordinate systems were used to clearly observe the behavior. The axial strain is the shortening strain and is selected to be a positive strain. The reason for this selection is to follow the conventional sign of strain in stress–strain models available in the literature. The lateral strain is the expansive strain and is thus selected to be negative. In Figure 10, the axial load–lateral strain curves were plotted on the negative side (the left side), while the axial load–axial strain curves were plotted on the positive side (the right side). Coordinates of the yield points and the ultimate points are shown, and their coordinates are used for analyses in the later sections.

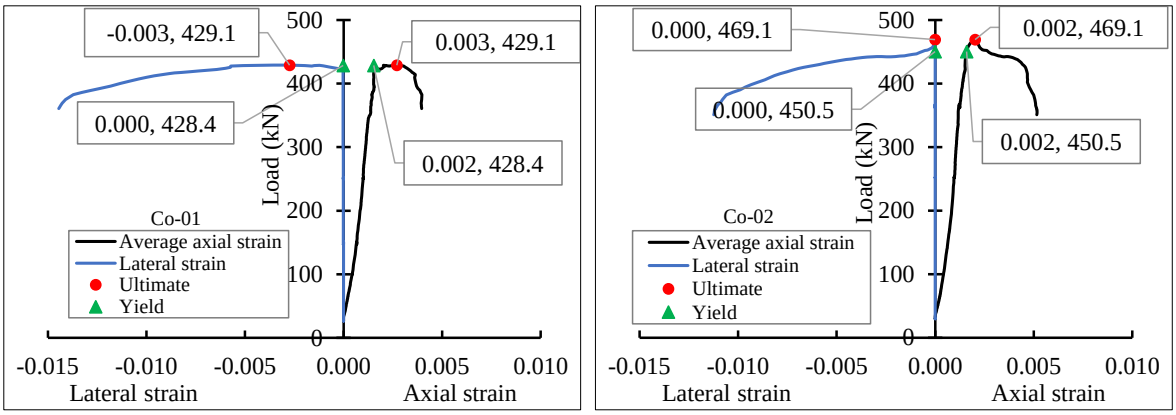

a) Co-01

b) Co-02

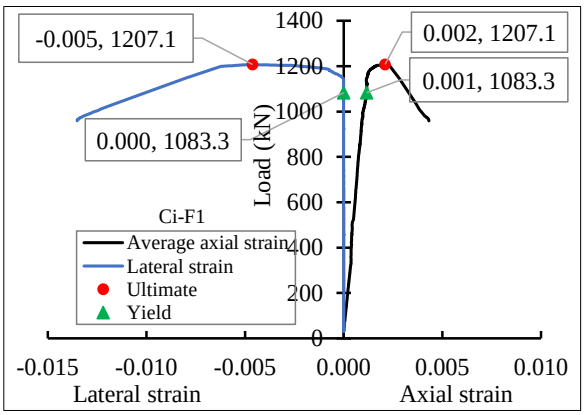

c) Ci-F1

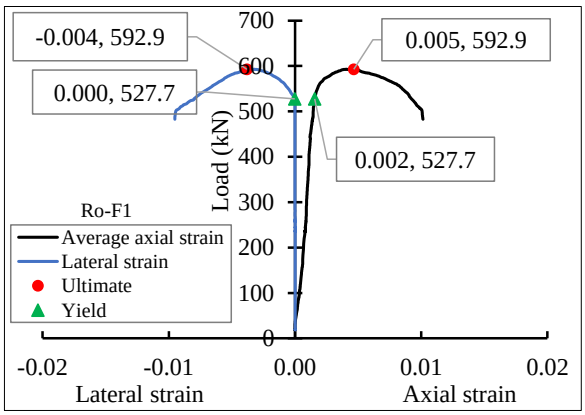

d) Ro-F1

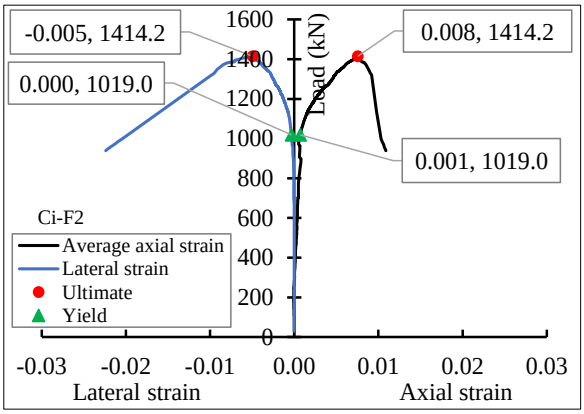

e) Ci-F2

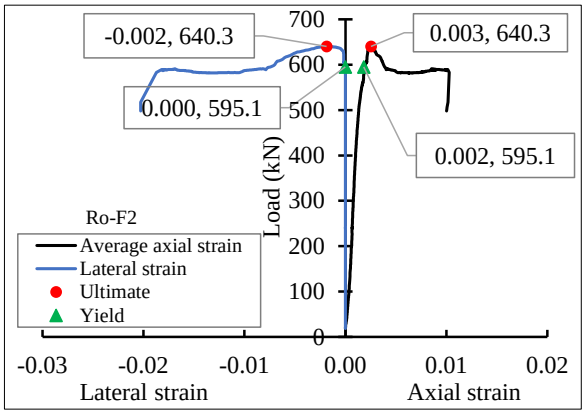

f) Ro-F2

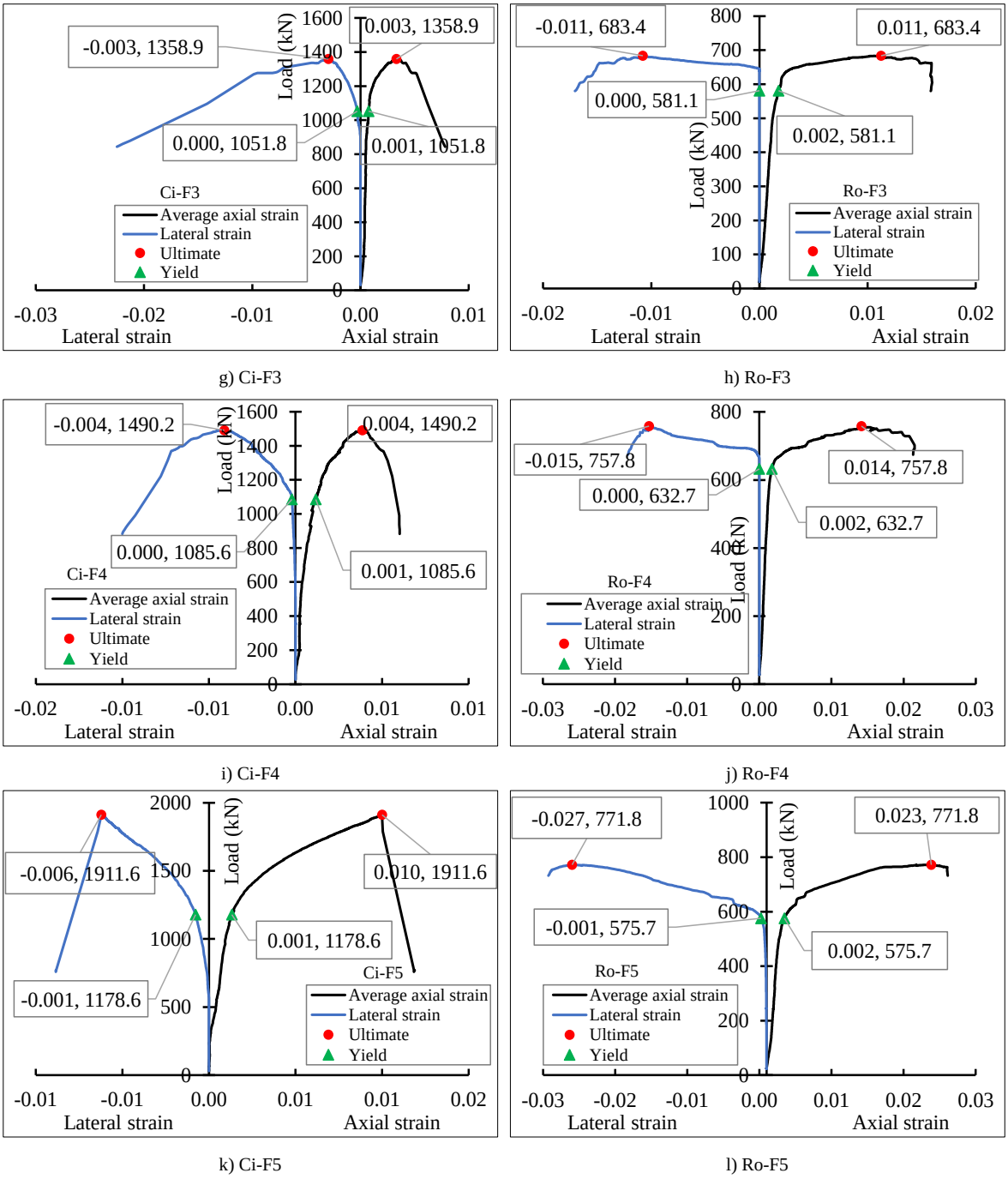

g) Ci-F3 h) Ro-F3

i) Ci-F4 j) Ro-F4

k) Ci-F5 l) Ro-F5

Figure 10. Axial load–strain curves

Figure 10 indicates that the load–strain behavior of columns under eccentric loading varied significantly. For control columns Co-01 and Co-02, the load–strain curves of the control columns exhibited a linear line up to the yield point and then immediately moved to the plastic and descending branch. The ultimate point is very close to the yield point. The loads of these two points are very close to each other. This behavior is also found for columns with low confinement Ro-F1 and Ci-F1, although the branch from yield to ultimate points is slightly longer. This shows the low ductility of the control columns and columns retrofitted with CFRP configuration F1.

The behavior of column Ro-F2 is also similar to the behavior described above, but with the following difference after the ultimate point: the load slightly decreased and then sustained at a certain load for a long domain of strain. This behavior indicates the effect of CFRP confinement. The post-yield branch of column Ro-F2 is governed by low confinement of one CFRP layer and stress concentration at column corners. In contrast, the behavior of column Ci-F2 is completely different from that of column Ro-F2, even though these two columns had the same configuration of one CFRP layer. The difference is that the load–strain curve of column Ci-F2 has a clear ascending branch after the yield point. This indicates the more effectiveness of the circularization, which eliminates the stress concentration as exhibited in column Ro-F2.

CFRP configuration F3 elongated both plastic branches of axial load–axial strain curves and the axial load–lateral strain curves of column Ro-F3. These elongations increased the ductility (Figure 10-h). In contrast, CFRP configuration

F3 shortened the plastic branches of column Ci-F3, reducing the ductility of this column. However, the slope of the plastic branch of column Ci-F3 is significantly higher than that of column Ro-F3. Additionally, the ultimate load of column Ci-F3 almost doubles that of column Ro-F3. These results indicate that the circularized method is very effective in increasing the load-carrying capacity and the plastic stiffness, whereas the ductility was reduced. The higher ductility of column Ro-F3 is explained by the fact that this column still has areas of unconfined concrete, which provides condition for axial shortening. The sections with one layer of CFRP seem to govern the ultimate points of columns retrofitted with configuration F3.

CFRP configuration F4 slightly improved the behavior, plastic stiffness, and load-carrying capacity of the columns. The phenomenon observed in these columns is almost similar to those of columns with the retrofitting configuration F3. This can be explained by the fact that sections with one CFRP layer still exist in these columns. These sections governed the failure mode and behavior of the columns. When all sections of columns were retrofitted by two CFRP layers of configuration F5, the behavior and load-carrying capacity of columns Ci-F5 and Ro-F5 increased significantly. The plastic stiffness of these columns also increased. These results are attributed to the fact that all sections are wrapped with two CFRP layers. The effectiveness of CFRP configuration retrofitting is significantly higher in column Ci-F5 than in column Ro-F5. The ultimate load of column Ci-F5 is more than double that of column Ro-F5.

An interesting point observed in Figure 10 is that the lateral strains at yield points are very close to zero. This is explained by the elastic behavior of the columns. In this elastic phase, the lateral expansion is obviously small. However, when the columns work in the plastic phase after the yield point, the lateral strain increases significantly. With the presence of CFRP confinement, the lateral strain of concrete is mitigated or partly prevented while the strain and ductility of concrete increase. As a result, the load–strain curve ascends in the range from the yield point up to the ultimate point. The ultimate is governed by the rupture failure of CFRP, which deactivates the confinement effect provided to concrete. Consequently, the high compression load damages the unconfined concrete, resulting in a sharp drop in load.

Figure 11 presents all load–strain curves in a coordinate system for comparisons. This figure clearly distinguishes these curves into three groups: 1) control group, 2) corner-rounded group, and 3) circularized group. The curves of control columns Co-01 and Co-02 were plotted in black color. The curves of CFRP-confined corner-rounded columns (Ro-F1–Ro-F5) and CFRP-confined circularized columns (Ci-F1–Ci-F5) were plotted in blue and red colors, respectively. The following observations can be made:

- The curves of control columns are the lowest, followed by those of CFRP-confined corner-rounded columns. The curves of CFRP-confined circularized columns (Ci-F1–Ci-F5) are the highest, showing an outstanding difference with the other two groups.
- With a similar configuration of CFRP wrapping, the ultimate loads of CFRP-confined corner-rounded RC columns are significantly lower than those of CFRP-confined circularized RC ones.
- On the axial load–lateral strain curves, the lateral strains of CFRP-confined corner-rounded RC columns are almost zero up to the yield point. After the yield point, the lateral strain increases significantly while the load increases slowly. This phenomenon creates a sharp transition from the elastic branch to the plastic branch. In contrast, the lateral strains of CFRP-confined circularized RC columns increase smoothly from the elastic branch to the plastic branch, probably due to the more uniform confining stress in these columns.
- The rupture of CFRP at a high ultimate load creates a sharp drop of load. This is because the rupture of CFRP deactivates the effect of confinement, changing confined concrete to unconfined concrete. Consequently, the unconfined concrete is unable to resist the load, leading to its failure. A high amount of energy is released, and the load drops sharply.

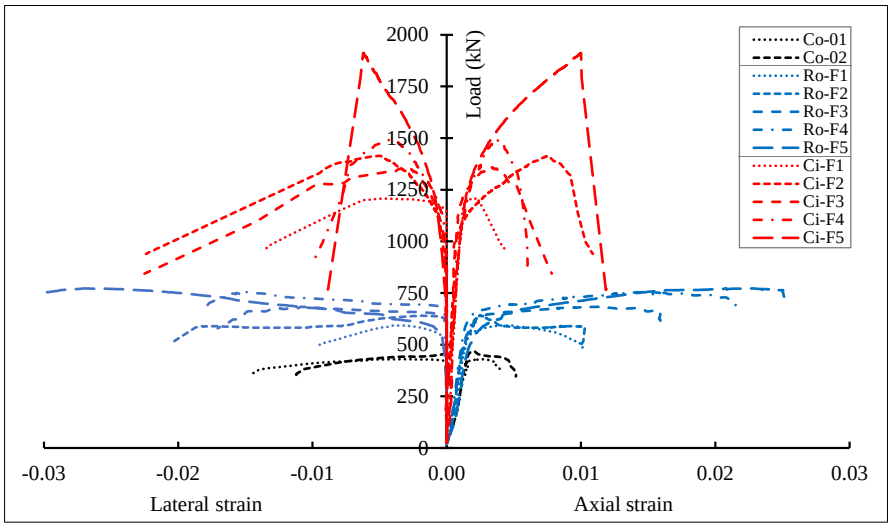

Figure 11. Comparison of axial load–strain curves

The elastic stiffness is defined by the slope of the branch from zero to the yield point (the elastic branch). Similarly, the plastic stiffness is defined by the branch from the yield point to the ultimate point (the plastic branch). Figure 11 also clearly indicates that the stiffness of the circularized columns is the highest, followed by the stiffness of CFRP-confined corner-rounded columns, whereas that of the control columns is the smallest. Additionally, the stiffness of CFRP-confined corner-rounded columns is very close to that of the control columns. These results indicate the greater effectiveness of CFRP confinement in the circularized columns than in the corner-rounded columns.

Overall, with a similar CFRP retrofitting configuration, the effectiveness of the circularization method is significantly higher than the corner-rounding method. The lateral strain in the range from zero to the yield point is almost zero. The lateral strain developed mainly in the plastic phase.

4. Analyses of the Experimental Results

4.1. Ultimate Loads

Figure 12-a plots the ultimate loads of all columns. Control RC columns Co-01 and Co-02 had the ultimate loads of 429.1 and 469.1 kN, respectively. Their average value is 449.1 kN, which is used for comparisons with other columns, as presented in Figure 12-b. The CFRP retrofitting configuration F1 increased the ultimate load of column Ro-F1 to 592.9 kN, which is 1.3 times the average ultimate load of the control columns. Further increasing the level of confinement to F2, F3, F4, and F5, the ultimate load of columns Ro-F2, Ro-F3, Ro-F4, and Ro-F5 slightly increased to 640.3, 683.4, 757.8, and 771.8 kN, which are 1.4, 1.5, 1.7, and 1.7 times the average ultimate load of the control columns. These results indicate that the presence of a small CFRP amount significantly changes the confinement status of the specimen from low/unconfined concrete to confined concrete, leading to a significant change in the load-carrying capacity. Further increasing the confinement only slightly improves the additional effectiveness. In spite of the significant change in the confinement from configuration F1 to configuration F5, the ultimate load varies slightly from 1.3 to 1.7, showing a low effectiveness in increasing the number of CFRP layers. This is a point that should be taken into account when designing the confinement for rectangular columns with the corner-rounding method.

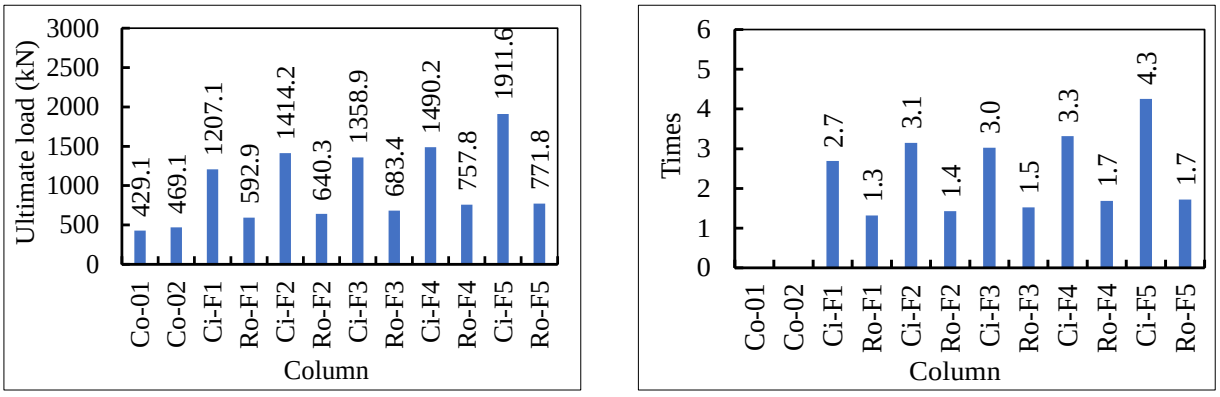

a) Ultimate loads b) Comparisons

Figure 12. Ultimate loads and comparisons

Differently, the circularization method outstandingly improves the effectiveness of CFRP wrapping. The CFRP retrofitting configuration F1 increased the ultimate load of column Ci-F1 to 1207.1 kN, which is 2.7 times the average ultimate load of the control columns and 2.0 times the ultimate load of the CFRP-confined corner-rounded column Ro-F1. These results confirm the direct and indirect contributions of the circularization to the ultimate load of the column. With one layer of CFRP wrapping, the ultimate load of column Ci-F2 increased to 1414.2 kN, which is 3.1 times the average ultimate load of the control columns. Similarly, CFRP retrofitting configurations F3 and F4 increased the ultimate loads of columns Ci-F3 and Ci-F4 to 1358.9 kN and 1490.2 kN, which are 3.0 and 3.3 times the average ultimate load of the control columns, respectively. Retrofitting configurations with 1.0, 1.33, and 1.67 CFRP layers increased a similar amount of the ultimate load. This can be explained by the fact that the eccentric loading caused the initial damage at the weaker section of one CFRP layer, while the damage did not initiate at sections with two CFRP layers. The configurations F2, F3, and F4 have the weakest section of one CFRP layer; therefore, these columns exhibited a similar ultimate load. Interestingly, retrofitting configuration F5 with two CFRP wrapping layers exhibited a difference. The retrofitted column Ci-F5 had the ultimate load of 1911.6 kN, which is 4.3 times the average ultimate load of the control columns. This is explained by the fact that all sections of the column were equally confined by two layers of CFRP. The damage initiated at an arbitrary point of the section and progressively expanded to a larger area of CFRP.

Overall, the corner-rounding method limitedly improved the ultimate load by 1.3–1.7 times. The differences in the improvement are marginal when the CFRP confinement stiffness increased from 0.33 to 2.0 layers. In contrast, the circularization method significantly improves the ultimate load by 2.7–4.3 times. The differences are very clear for 0.33 CFRP layer (2.7 times), 1.0–1.67 layers (3.0–3.3 times), and 2.0 layers (4.3 times). With a similar CFRP configuration, the ratio of the ultimate load of the CFRP-confined circularized column to that of the CFRP-confined corner-rounded column can be defined for additional comparisons. These ratios are 2.04, 2.21, 1.99, 1.97, and 2.48 for CFRP configurations F1, F2, F3, F4, and F5, respectively. The average ratio is 2.14, which demonstrates the high efficiency of the circularization method compared with the corner-rounding method. The direct contribution of the circularization method is the increase in the concrete area, while its indirect contribution is the improvement in the effectiveness of CFRP wrapping by mitigating or partly preventing the stress concentration at column corners.

4.2. Ultimate Rotations

Under eccentric loading, the two measured sections relatively rotated with respect to each other. The ultimate rotations were determined and then plotted in Figure 13-a. Control columns Co-01 and Co-02 had the ultimate rotations of 0.017 and 0.009 rad, respectively. Figure 13-b shows comparisons of the ultimate rotations of other columns with the average value of 0.013 rad of the control columns. For CFRP configurations F1 and F2, the ultimate rotation of the corner-rounded column is lower than that of the circularized column with the same CFRP configuration. The ultimate rotations of circularized columns Ci-F1 and Ci-F2 are 0.023 and 0.039 rad, which are 76.9% and 200% higher than that of the control columns, respectively. The ultimate rotations of corner-rounded columns Ro-F1 and Ro-F2 are 0.012 and 0.020 rad, which are 7.7% lower and 53.8% higher than that of control columns, respectively.

The increase and the difference in the ultimate rotations become significant for columns with higher CFRP confinement configurations F3–F5. The ultimate rotations of columns Ci-F3, Ci-F4, and Ci-F5 are 0.035, 0.046, and 0.078 rad, which are 169.2%, 253.8%, and 500% higher than the ultimate rotation of the control columns, respectively. The ultimate rotations of columns Ro-F3, Ro-F4, and Ro-F5 are 0.067, 0.102, and 0.143 rad, which are 415.4%, 684.6%, and 1000% higher than the ultimate rotation of the control columns, respectively. Therefore, the ultimate rotation of a corner-rounded column is higher than that of a circularized column when they have the same CFRP configuration. Additionally, the ultimate rotation increased with the increase in the confinement stiffness. This is attributed to the fact that the higher confinement stiffness can mitigate the local damage of concrete, delaying the rupture failure of CFRP.

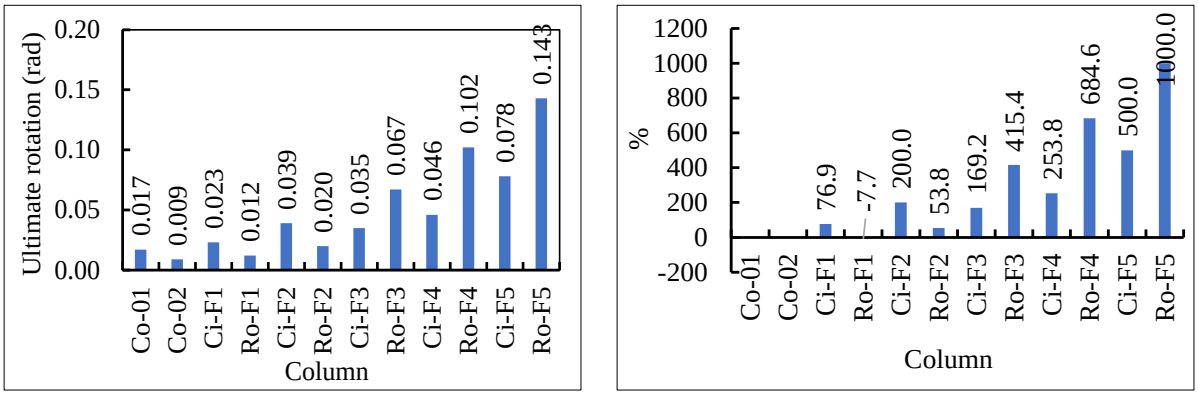

a) Ultimate rotations b) Comparisons

Figure 13. Ultimate rotations

4.3. Ultimate Axial Strains

Ultimate axial strains of the tested columns are plotted in Figure 14-a. Figure 14-b compares the ultimate axial strains with the average axial strain of control columns. Overall, the ultimate axial strains tend to increase with the increase in the confinement stiffness of CFRP wrapping. The ultimate lateral strains of control columns Co-01 and Co-02 are 2.7×10^{-3} and 2.0×10^{-3}, respectively. Their average value is 2.35×10^{-3}, which is used for comparisons. The ultimate lateral strains of the corner-rounded columns vary significantly from 2.5×10^{-3} to 22.8×10^{-3}, which are 6.4–870.2% higher than the average ultimate strain of control columns. The ultimate lateral strains of the CFRP-confined circularized columns vary significantly from 2.1×10^{-3} to 10.0×10^{-3}, which are -10.6–325.5% higher than the ultimate strain of control columns. Except for the CFRP configuration F2, the CFRP-confined circularized column has lower ultimate axial strains than the CFRP-confined corner-rounded column when they have the same CFRP retrofitting configuration. This is attributed to the ineffective regions and stress concentration in CFRP-confined corner-rounded columns.

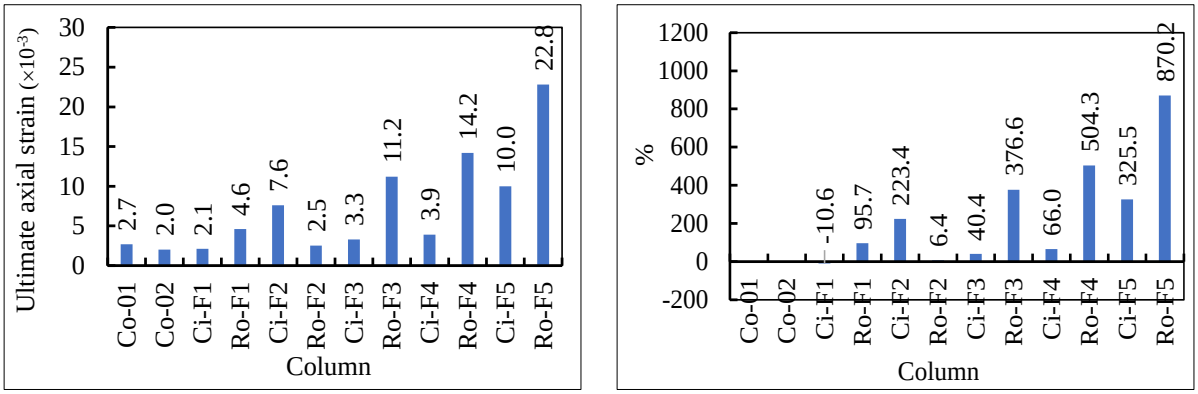

a) Ultimate axial strains b) Comparisons

Figure 14. Ultimate axial strains and comparisons

4.4. Ultimate Lateral Strain

The lateral strain can be marginal during the elastic phase while it develops significantly during the plastic phase. The ultimate lateral strains of the tested columns are shown in Figure 15-a, and their comparisons with the average ultimate strain of control columns are presented in Figure 15-b. Control column Co-01 has the ultimate lateral strain of 2.734×10^{-3}, while control column Co-02 has the ultimate strain of 0.001×10^{-3}. The small ultimate lateral strain of column Co-02 is probably due to the local damage of concrete at corners. However, it may represent the lower bound of the ultimate lateral strain. Thus, the average ultimate lateral strain of 1.368×10^{-3} can be used for comparisons, as presented in Figure 15-b. With low CFRP confinement configurations F1 and F2, the ultimate lateral strains of corner-rounded columns are lower than those of circularized columns. Compared with the average ultimate lateral strain of the control columns, the lateral strains of columns with CFRP configurations F1 and F2 increased by 35–263%.

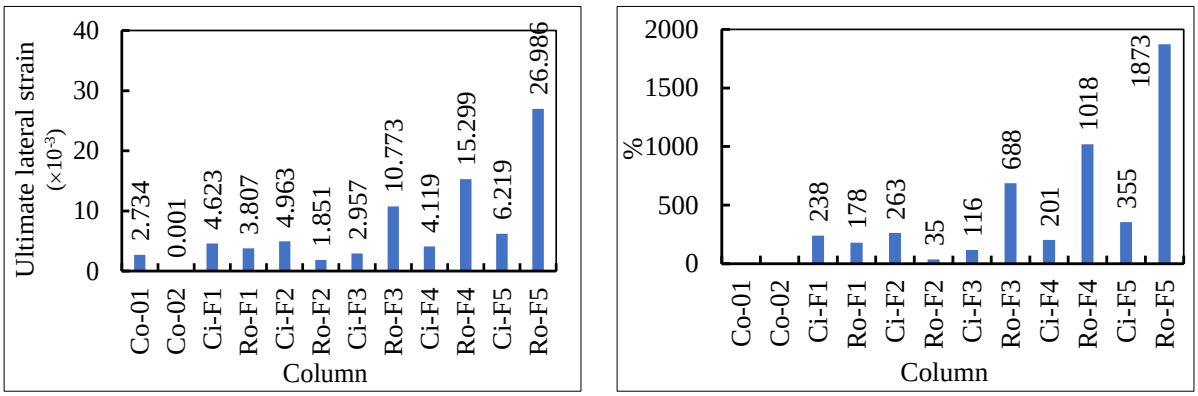

a) Lateral strains b) Comparisons

Figure 15. Lateral strains and comparisons

For higher confinement configurations F3–F5, the ultimate lateral strains of CFRP-confined circularized columns are significantly lower than those of CFRP-confined corner-rounded columns. Additionally, the ultimate lateral strain increases with the increase in the confinement stiffness. Compared with the average ultimate lateral strain of the control columns, the lateral strains of circularized columns Ci-F3, Ci-F4, and Ci-F5 increased by 116%, 201%, and 355%, while those of columns Ro-F3, Ro-F4, and Ro-F5 increased by 688%, 1018%, and 1873%, respectively. The phenomena: 1) the increase in the ultimate lateral strain with the increase in the confinement stiffness, and 2) the higher ultimate lateral strain of the corner-rounded column compared with that of the circularized column with the same CFRP configuration, are similar to those of the ultimate axial strains.

4.5. Yield Load

Figure 16-a presents the yield loads of the tested columns. Control columns Co-01 and Co-02 had yield loads of 428.4 kN and 450.5 kN, respectively. The average yield load of control columns was 439.45 kN. Comparisons of the yield loads of other columns with the average yield load of control columns are presented in Figure 16-b. CFRP retrofitting slightly increased the yield load of CFRP-confined corner-rounded columns to 527.7–632.7 kN, which is 1.2–1.4 times (1.3 times on average) that of the control columns. With the circularization method, CFRP wrapping significantly increased the yield load to 1019.0–1178.6 kN, which is 2.3–2.7 times (2.48 times on average) that of the

control columns. The circularization, regardless of the CFRP confinement stiffness, significantly changed the yield load of CFRP-confined circularized columns. Another characteristic is that the yield load marginally varies with the variation in confinement stiffness. One of the reasons is that the yield load is located at the end of the elastic branch, at which the confinement starts to work due to its passive confinement.

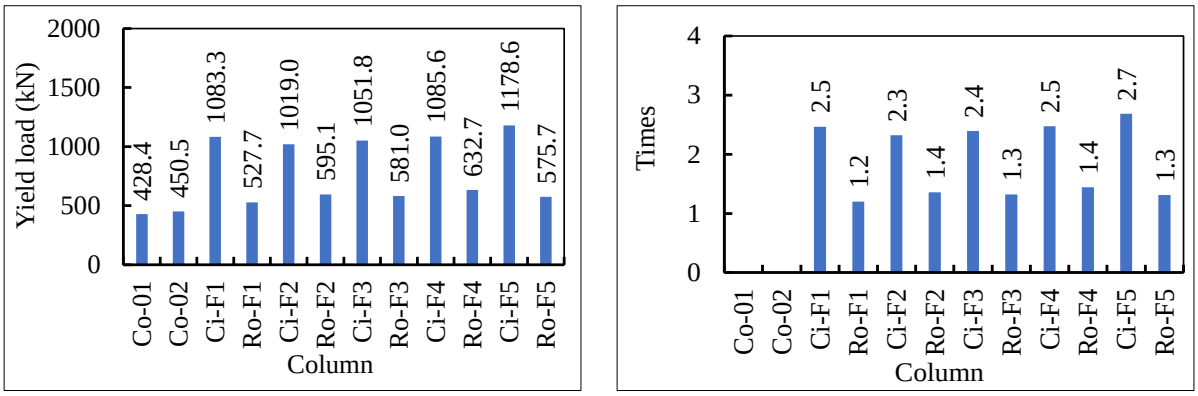

a) Yield loads b) Comparisons

Figure 16. Yield loads

4.6. Yield Axial Strains

The yield axial strain is defined by the point where the load–axial strain curves start to deviate from the linear branch. The yield axial strains of the tested columns are plotted in Figure 17-a. The control columns Co-01 and Co-02 had the axial yield strains of 1.5×10^{-3} and 1.6×10^{-3}, respectively. With the presence of CFRP configuration F1, the yield strain of CFRP-confined circularized RC column Ci-F1 decreased to 1.2×10^{-3}, while that of the CFRP-confined corner-rounded column Ro-F1 remained at 1.6×10^{-3}. When CFRP configuration increased to F2, the yield axial strain of the corner-rounded column increased to 1.8×10^{-3}, which remained the same for columns with configurations F3 and F4. CFRP-confined corner-rounded column Ro-F5 had the highest yield axial strain of 2.5×10^{-3}. For CFRP-confined circularized RC columns, the yield strain varied from 0.7×10^{-3} to 1.3×10^{-3}, which are overall lower than those of the CFRP-confined corner-rounded columns. Compared with the yield axial strains of control columns, the yield axial strain of corner-rounded columns increases by up to 16.1–61.3%, whereas those of circularized RC columns decrease by up to 16.1–54.8%, as shown in Figure 17-b. This can be explained by the more uniform confinement in the circularized columns. In contrast, CFRP-confined corner-rounded columns still had four unconfined areas at the four sides of the columns.

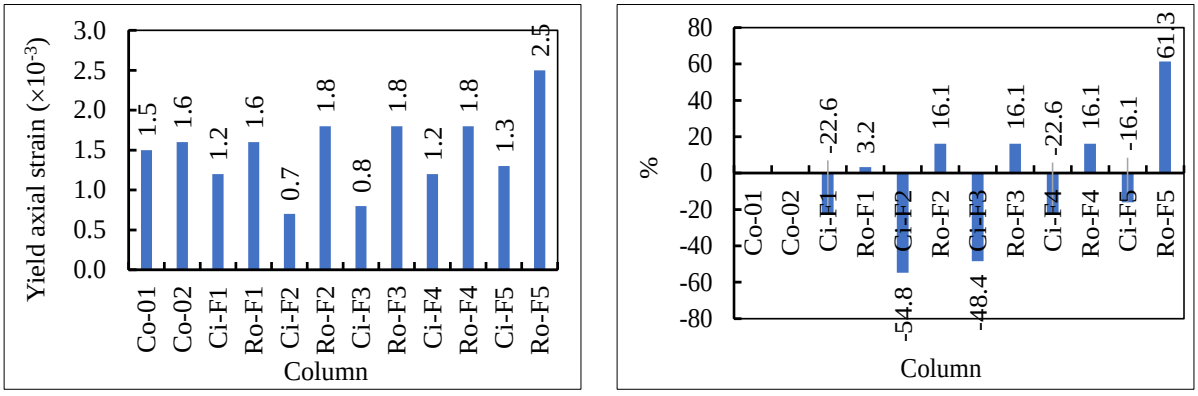

a) Yield axial strains b) Comparisons

Figure 17. Yield axial strains

4.7. Yield Rotations

Yield rotations of the tested columns are presented in Figure 18-a. Control columns Co-01 and Co-02 had the yield rotations of 0.007 and 0.006 rad, respectively. Their average value is 0.0065 rad, which is used to compare with those of other columns, as presented in Figure 18-b. The CFRP-confined corner-rounded column Ro-F1 had the yield rotation of 0.06 rad, which increased to 0.011–0.014 rad for CFRP-confined columns with CFRP retrofitting configurations F2–F5. Compared with the yield rotation of control columns, yield rotations of columns Ro-F2–Ro-F5 increased up to 57.1%–100%. Similarly, the yield rotation of CFRP-confined circularized columns Ci-F2–Ci-F5 varied between 0.008

and 0.012 rad, which are 14.3%–71.4% higher than that of the control columns. Generally, the presence of CFRP confinement increased the yield rotation, while yield rotation slightly varies when the confinement level varies from one layer to two layers of CFRP.

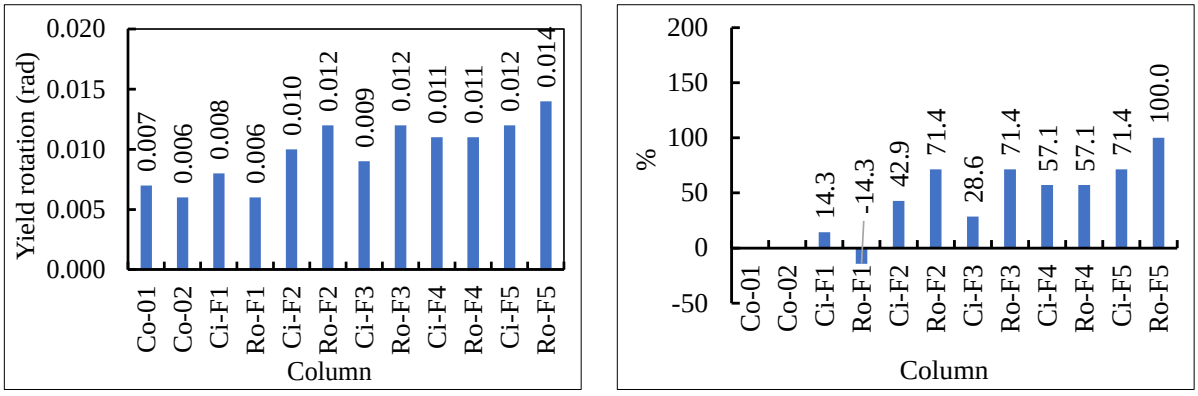

a) Yield rotations b) Comparisons

Figure 18. Yield rotations

4.8. Rotation Ductility

Rotation ductility of columns under eccentric loadings is defined by the ratio of the ultimate rotation (Section 4.2) to the yield rotation (Section 4.7). Their rotation ductility was computed and plotted in Figure 19-a while comparisons are shown in Figure 19-b. The control columns Co-01 and Co-02 have the rotation ductility of 2.4 and 1.5, which are 1.95 on average and considered to be low ductile. CFRP configuration F1 slightly improved the rotation ductility of columns Ci-F1 and Ro-F1 to 2.9 and 2.0 (moderate ductile), respectively. When confinement increased to one CFRP layer (configuration F2), the rotation ductility of column Ci-F2 increased to 3.9 (moderate ductile), whereas the rotation ductility of column Ro-F2 was 1.7, which is considered to be low ductile. Further increasing the confinement stiffness, the rotation ductility of CFRP-confined corner-rounded and circularized columns increased up to 10.2 and 6.5, respectively. Overall, CFRP confinement provides higher rotation ductility for eccentrically loaded columns. This can be explained by the fact that the presence of CFRP confinement prevents the lateral strain for concrete, improves the lateral strain capacity, and improves the axial strength and strain of concrete. Consequently, the failure of concrete was delayed, which, in turn, increased the ultimate axial strain of the columns.

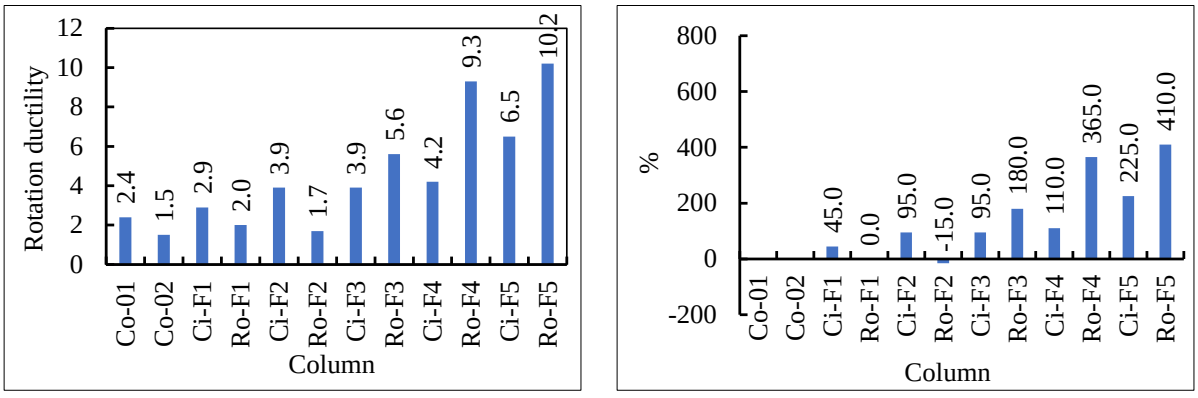

a) Rotation ductility b) Comparisons

Figure 19. Rotation ductility

4.9. Elastic Stiffness

The elastic stiffness of the tested columns is defined by the slope of the load–strain curves up to the yield points. The elastic stiffness was determined in Excel, with the coefficient of determination (R^2) larger than 0.81, and the results are shown in Figure 20-a. Control columns Co-01 and Co-02 had the elastic stiffness of 260.6×10^3 and 280.4×10^3 kN/strain, respectively. Their average value is 270.5×10^3 kN/strain, which is used for comparisons with the elastic stiffness of other columns, as presented in Figure 20-b. The elastic stiffness of corner-rounded columns with different retrofitting configurations varied from 266.0×10^3 kN/strain to 429.9×10^3 kN/strain, which corresponds to 1.7% lower and 58.9% higher than the elastic stiffness of control columns. Thus, CFRP wrapping with corner rounding seems to negligibly increase/decrease the elastic stiffness of the columns. This is attributed to the fact that CFRP confinement

does not change the elastic stress–strain behavior of CFRP-confined concrete compared with unconfined concrete, as evidenced in the Lam & Teng's [25, 26] model. Lam & Teng [25, 26] model indicates that the stress–strain behavior of CFRP-confined concrete only slightly elongates the elastic branch while it significantly improves the plastic branch.

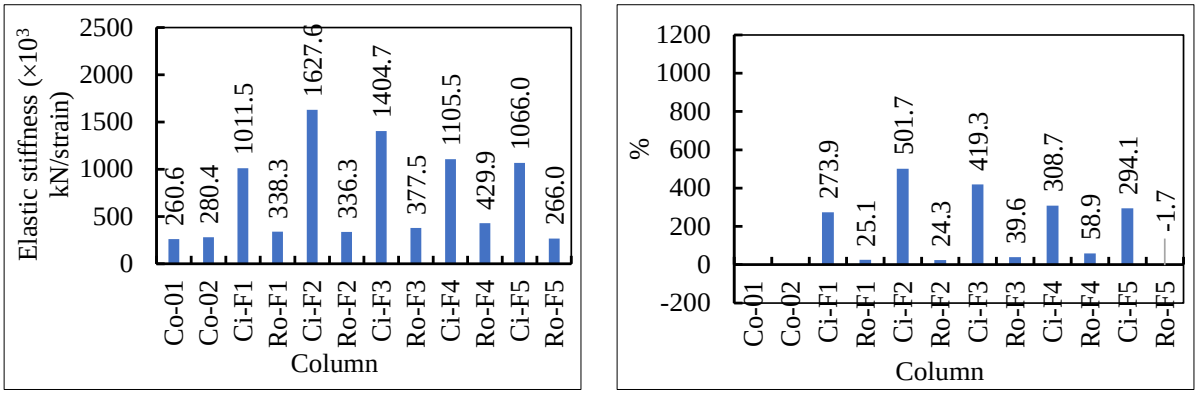

a) Elastic stiffness b) Comparisons

Figure 20. Elastic stiffness

In contrast, the elastic stiffness of CFRP-confined circularized RC columns increased significantly to 1066.0×10^3–1627.6×10^3 kN/strain, which corresponds to 294.1%–501.7% higher than that of control columns. This significant increase in the elastic stiffness of the CFRP-confined circularized RC column is explained by the increase in its concrete section (the circularized concrete). It is noted that the increase in the elastic stiffness may be marginally contributed by the CFRP confinement, as explained in the previous paragraph.

4.10. Plastic Stiffness

Plastic stiffness is defined as the slope of the branch from the yield point to the ultimate point. The plastic stiffness was determined in Excel, with R^2 larger than 0.81. Figure 21-a shows the plastic stiffness of the tested columns, while comparisons are presented in Figure 21-b. The plastic stiffness of the control column Co-01 was 4.9 kN/strain, whereas the second control column Co-02 had the plastic stiffness of 41.1 kN/strain. The relatively high plastic stiffness of the second control column is attributed to the short branch from the yield point to the ultimate point. The average plastic stiffness of the two control columns Co-01 and Co-02 is 23.0 kN/strain.

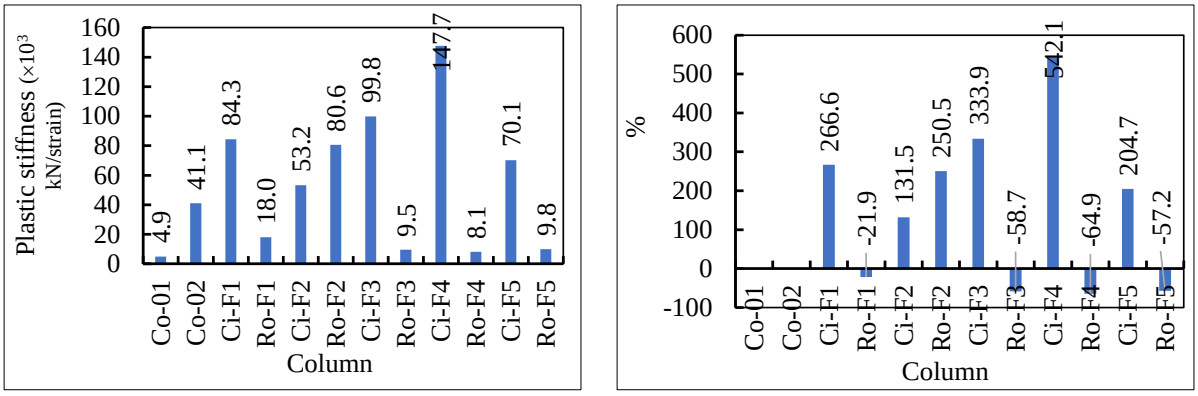

a) Plastic stiffness b) Comparisons

Figure 21. Plastic stiffness

Compared with the average plastic stiffness of the control specimens, the plastic stiffness of CFRP-confined corner-rounded columns Ro-F1 significantly increased to 84.3 kN/strain, which is 266.6% higher than the average plastic stiffness of control columns. However, when further increasing the stiffness of CFRP wrapping to configuration F2, the plastic stiffness of column Ro-F2 increased to 80.6 kN/strain. Further increasing the stiffness of CFRP wrapping configurations F3–F5, the plastic stiffness significantly decreased to 8.1–9.5 kN/strain, which is 64.9–58.7% lower than the plastic stiffness of the control columns. The decrease in the plastic stiffness of the control columns is explained by the fact that CFRP wrapping of corner-rounded columns significantly elongated the plastic branch. Specifically, CFRP wrapping of corner-rounded columns significantly increased the ultimate strain, whereas it slightly increased the ultimate load.

Moving on to the plastic stiffness of CFRP-confined circularized RC columns, CFRP configuration F1 increased the plastic stiffness of column Ci-F1 to 84.3 kN/strain, which is 266.6% higher than the average plastic stiffness of the control specimens. The plastic stiffness of column Ci-F2 was 53.2 kN/strain, which was then slightly decreased to 99.8, 147.7, and 70.1 kN/strain for columns Ci-F3, Ci-F4, and Ci-F5, respectively. The configuration F4 resulted in the highest plastic stiffness for column Ci-F4, which is 542.1% higher than the average plastic stiffness of the control specimens. These increases in the plastic stiffness demonstrate that CFRP wrapping provides high confinement effectiveness to the circularized concrete.

5. Theoretical Analyses

5.1. Theoretical Background

In this subsection, a theory of rectangular and circular RC columns subjected to an eccentric load N with the eccentricity of e (Figure 22-a) is presented. These eccentrically loaded columns are similar to the case of the same columns subjected to a concentric load N and a moment M, in which $M = N \times e$, as shown in Figure 22-b. The stress caused by this load combination is calculated by Equation 4, in which A is the cross-sectional area and W is the sectional modulus of the cross section. For rectangular sections, A and W are determined by Equations 5 and 6, respectively, in which b and h are the width and the height of the cross section. For circular sections, A and W are determined by Equations 7 and 8, respectively, in which R is the radius of the cross section.

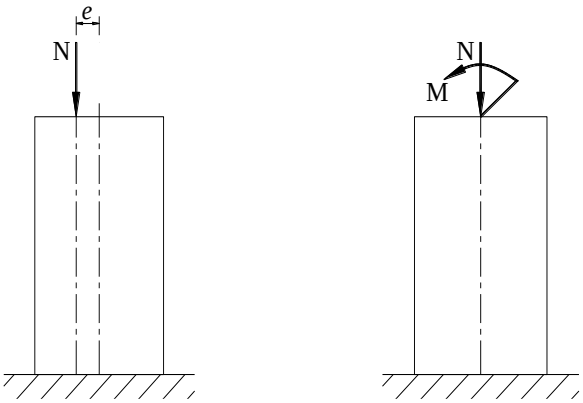

a) Compression load N with eccentricity e b) Concentric load N and moment M

Figure 22. Columns under eccentric loads

$$\sigma_{max} = \frac{N}{A} + \frac{M}{W} = \frac{N}{A} + \frac{Ne}{W} = \frac{N}{A}\left(1 + \frac{eA}{W}\right) \quad (4)$$

$$A = b \times h \quad (5)$$

$$W = \frac{b \times h^2}{6} \quad (6)$$

$$A = \pi \times R^2 \quad (7)$$

$$W = \frac{\pi \times R^3}{2} \quad (8)$$

Substituting Equations 5 and 6 into Equation 4, Equation 9 is obtained to calculate the maximum stress for rectangular columns. Substituting Equations 7 and 8 into Equation 4, Equation 10 is obtained to calculate the maximum stress for circular columns.

$$\sigma_{max} = \frac{N}{bh}\left(1 + \frac{6e}{h}\right) \quad (9)$$

$$\sigma_{max} = \frac{N}{\pi R^2}\left(1 + \frac{2e}{R}\right) \quad (10)$$

At the ultimate, the stress of the extreme fiber of concrete can be taken as the ultimate strength of confined concrete f'_{cu}. Substituting $\sigma_{max} = f'_{cu}$ and rearranging Equations 9 and 10, Equations 11 and 12 are obtained and used to calculate the ultimate loads for rectangular and circular sections, respectively.

$$N = \frac{f'_{cu} bh}{1+\frac{6e}{h}} \quad (11)$$

$$N = \frac{\pi R^2 f'_{cu}}{1+\frac{2e}{R}} \quad (12)$$

For the tested control and corner-rounded columns, e = 50 mm = h/4, b = 150 mm, and h = 200 mm. For circularized columns, R = 267/2 mm = 133.5 mm.

The ultimate strength of concrete f'_{cu} for control columns can be taken as the compressive strength of concrete cylinder samples. This is because the unconfined concrete at the extreme fiber of control columns crushed at the ultimate state. The ultimate strengths of CFRP-confined rectangular and circular concrete columns are presented in the following sections.

5.2. Ultimate Strength of FRP-Confined Concrete

Several stress–strain models of the ultimate strength of FRP-confined concrete are available in the literature. Among these models, the Lam & Teng [25, 26] models are appropriate for both circular and rectangular concrete columns, as commented by Rocca et al. [51]; therefore, these models were adopted in ACI 440.2R-08 [52]. Details of Lam & Teng [25, 26] models are presented in Lam & Teng [25, 26], while only the ultimate compressive strengths f'_{cu} of circular and rectangular concrete columns confined by CFRP are presented herein.

For rectangular cross-sectional concrete, ultimate strengths are calculated by Equation 13 or 14, depending on the ratio of confined stress f_{la} to the concrete strength f'_c compared with the value 0.07. The confined stress f_{la} is determined by Equation 15, in which t_f is the CFRP thickness, $\varepsilon_{h,rup}$ is the rupture strain of CFRP, E_f is the modulus of CFRP, $E_c = 4730\sqrt{f'_c}$ [53] is the modulus of concrete, and D is the equivalent diameter determined by Equation 16. k_{s1} is the shape factor determined by Equation 17, followed by Equation 18, where r is the corner-rounded radius and ρ_s is the ratio of longitudinal steel.

$$f'_{cu} = f'_c \left[1 + 3.3 k_{s1} \frac{f_{la}}{f'_c}\right] \quad \text{if} \quad \frac{f_{la}}{f'_c} \geq 0.07 \quad (13)$$

$$f'_{cu} = f'_c \quad \text{if} \quad \frac{f_{la}}{f'_c} < 0.07 \quad (14)$$

$$f_{la} = \frac{\varepsilon_f \tau_f}{R} \varepsilon_{h,rup} = \frac{2\varepsilon_f \tau_f}{D} \varepsilon_{h,rup} \quad (15)$$

$$D = \sqrt{h^2 + b^2} \quad (16)$$

$$k_{s1} = \left(\frac{b}{h}\right)^2 \frac{A_e}{A_c} \quad (17)$$

$$\frac{A_e}{A_c} = \frac{1-((b/h)(h-2r)^2+(h/b)(b-2r)^2)/(3A_g)-\rho_s}{1-\rho_s} \quad (18)$$

For circular cross sections of concrete, Equations 13–15 are used while the shape factor k_{s1} is taken as 1.0. R is the diameter of cross sections.

$\varepsilon_{h,rup}$ is the rupture strain of CFRP, which is calculated by $\varepsilon_{h,rup} = K_\varepsilon \varepsilon_{frp}$. k_ε is 'FRP strain efficiency factor' and ε_{frp} is the rupture strain of CFRP. Different values for k_ε have been proposed by researchers based on different databases. Based on test results of 52 CFRP wrapped specimens, Lam & Teng [25] proposed k_ε = 0.586. ACI 440.2R-08 [52] used k_ε = 0.55. Based on 62 test results, Realfonzo & Napoli [54] proposed k_ε = 0.63. Using 661 FRP (477 CFRP and 184 GFRP) wrapped specimens, Baji [55] proposed k_ε = 0.62. Using 509 test results of specimens wrapped with only CFRP, Baji et al. [56] found k_ε = 0.68, which is the most updated value and is very close to the value of 0.7 determined by Pham et al. [43]. Thus, it is used in this study.

5.3. Calculation Results and Comparisons

Calculation results of ultimate loads are presented in column 5 of Table 3 in comparison with those obtained from the experiments. The differences between these two results are presented in the last column of Table 3. The comparison results showed that the proposed method underestimates the ultimate load of CFRP-confined corner-rounded columns. The underestimation varies from 7.4% to 17.7% compared with the experimental results. The proposed method underestimates the ultimate load of CFRP-confined circularized columns Ci-F1 and Ci-F5 by 8.1% and 6.5%, respectively, while it accurately estimates that of column Ci-F2. In contrast, the proposed method overestimates the ultimate load of CFRP-confined circularized columns Ci-F3 and Ci-F4 by 14.8% and 14.2%, respectively. Overall, the proposed models reasonably estimate the ultimate load of CFRP-confined circularized or corner-rounded RC columns.

Table 3. Calculation results and comparisons

No.	Column	Shape	Ultimate load (kN)		Difference (%)
			Experiment	Analysis	
(1)	(2)	(3)	(4)	(5)	(6)
1	Co-01	Control	429.1	547.1	21.8
2	Co-02	Control	469.1		
3	Ci-F1	Circularized	1207.1	1109.1	-8.1
4	Ro-F1	Corner-rounded	592.9	547.1	-7.7
5	Ci-F2	Circularized	1414.2	1448.3	2.4
6	Ro-F2	Corner-rounded	640.3	592.9	-7.4
7	Ci-F3	Circularized	1358.9	1560.2	14.8
8	Ro-F3	Corner-rounded	683.4	608.0	-11.0
9	Ci-F4	Circularized	1490.2	1675.5	12.4
10	Ro-F4	Corner-rounded	757.8	623.5	-17.7
11	Ci-F5	Circularized	1911.6	1787.5	-6.5
12	Ro-F5	Corner-rounded	771.8	638.6	-17.3

6. Conclusions

The following conclusions are drawn:

- CFRP-confined circularized RC columns failed by CFRP rupture at the eccentric side with weak to moderate explosions, while CFRP-confined corner-rounded RC columns failed by CFRP rupture localized at corners with weak explosions. The weak and moderate explosions are attributed to a combination of 1) the presence of internal steel, which mitigates the brittle failure, and 2) the eccentric loading, which prevents the failure at the same time.
- The outstanding effectiveness of the circularization method is its increase in the ultimate load of CFRP-confined circularized RC columns by 3.0–4.3 times that of the control columns, although the number of CFRP layers was varied only from 1 layer to 2 layers. In contrast, the corner-rounding method moderately increased the ultimate load of CFRP-confined corner-rounded RC columns by 1.3–1.7 times that of the control columns. These results confirm the superiority of the circularization method before CFRP wrapping.
- The ultimate lateral strains, ultimate axial strains, and ultimate rotations of CFRP-confined circularized RC columns are generally lower than those of CFRP-confined corner-rounded RC columns. This is attributed to the more uniform confining stress in CFRP-confined circularized RC columns. The rotation ductility of CFRP-confined circularized and corner-rounded RC columns significantly improves to high ductility when confined with more than 1.33 CFRP layers.
- The circularization method outstandingly improves the elastic stiffness by 273.9%–419.3% compared with that of control columns, due to the increase in the area of circularized concrete. In contrast, the corner-rounding method exhibits no effect on the elastic stiffness. This is attributed to the fact that CFRP confinement does not change the elastic stress–strain behavior of CFRP-confined concrete compared with unconfined concrete. CFRP confinement significantly improves the plastic stiffness of circularized RC columns, whereas it marginally changes the plastic stiffness of corner-rounded RC columns. This is attributed to the ineffective regions and stress concentration at corners in CFRP-confined corner-rounded RC columns.
- A simple calculation method was developed while Lam & Teng's [25, 26] models for the ultimate stress of FRP-confined concrete were adopted as the ultimate condition. Lam & Teng models were adopted with an assumption that the circularized and original concrete formed monolithic concrete. Additionally, the resistance contributed by the longitudinal steel was taken into account while the internal steel confinement was ignored. These assumptions compensate for each other because the confinement provided by internal steel may slightly contribute to the load-carrying capacity, whereas the longitudinal steel may not reach its ultimate strength. The proposed model demonstrates well in estimating the ultimate load-carrying capacity of CFRP-confined circularized and corner-rounded columns.

7. Declarations

7.1. Author Contributions

Conceptualization, T.D.D., C.T.N., and V.V.C.; methodology, T.D.D., C.T.N., and V.V.C.; validation, T.D.D. and V.V.C.; formal analysis, T.D.D. and V.V.C.; investigation, T.D.D. and V.V.C.; resources, T.D.D.; data curation, T.D.D. and V.V.C.; writing—original draft preparation, V.V.C.; writing—review and editing, T.D.D. and C.T.N.; visualization, T.D.D. and C.T.N.; supervision, T.D.D.; project administration, T.D.D.; funding acquisition, T.D.D. All authors have read and agreed to the published version of the manuscript.

7.2. Data Availability Statement

The data presented in this study are available in the article.

7.3. Funding

This research is funded by Vietnam National University HoChiMinh City (VNU-HCM) under grant number: B2024-20-09.

7.4. Conflicts of Interest

The authors declare no conflict of interest.

8. References

[1] Reda, R. M., Sharaky, I. A., Ghanem, M., Seleem, M. H., & Sallam, H. E. M. (2016). Flexural behavior of RC beams strengthened by NSM GFRP Bars having different end conditions. Composite Structures, 147(Supplement C), 131–142. doi:10.1016/j.compstruct.2016.03.018.

[2] Haddad, R. H., & Harb, A. N. (2022). Varying Profiles of CFRP Ropes for Strengthening Concrete Beams. International Journal of Civil Engineering, 20(4), 405–419. doi:10.1007/s40999-021-00664-2.

[3] Van Cao, V. (2024). Performance of NSM GFRP Retrofitted Postfire RC Slabs Under Monotonic and Cyclic Loadings. Civil Engineering Journal (Iran), 10(6), 1987–2006. doi:10.28991/CEJ-2024-010-06-017.

[4] Islam, M. R., Mansur, M. A., & Maalej, M. (2005). Shear strengthening of RC deep beams using externally bonded FRP systems. Cement and Concrete Composites, 27(3), 413–420. doi:10.1016/j.cemconcomp.2004.04.002.

[5] Saadah, M., Ashteyat, A., & Murad, Y. (2021). Shear strengthening of RC beams using side near surface mounted CFRP ropes and strips. Structures, 32, 380–390. doi:10.1016/j.istruc.2021.03.038.

[6] Nanda, R. P., & Behera, B. (2020). Experimental Study of Shear-Deficient RC Beam Wrapped with GFRP. International Journal of Civil Engineering, 18(6), 655–664. doi:10.1007/s40999-020-00498-4.

[7] Mercimek, Ö., Anıl, Ö., Akkaya, S. T., Erdem, R. T., Çelik, A., Kopraman, Y., & Abukan, A. (2025). Experimental behavior of shear deficient RC beams strengthened with CFRP strips againts reversible cylic earthquake load. Structural Concrete. doi:10.1002/suco.202401066.

[8] Eslami, A., & Ronagh, H. R. (2013). Effect of FRP wrapping in seismic performance of RC buildings with and without special detailing - A case study. Composites Part B: Engineering, 45(1), 1265–1274. doi:10.1016/j.compositesb.2012.09.031.

[9] Khan, A. R., Nasir, R., & Fareed, S. (2023). Simulation of Reinforced Concrete Columns Strengthened with CFRP Wraps. International Journal of Civil Engineering, 21(2), 299–313. doi:10.1007/s40999-022-00768-3.

[10] Khaloo, A., Tabatabaeian, M., & Khaloo, H. (2020). The axial and lateral behavior of low strength concrete confined by GFRP wraps: An experimental investigation. Structures, 27, 747–766. doi:10.1016/j.istruc.2020.06.008.

[11] Norris, T., Saadatmanesh, H., & Ehsani, M. R. (1997). Shear and Flexural Strengthening of R/C Beams with Carbon Fiber Sheets. Journal of Structural Engineering, 123(7), 903–911. doi:10.1061/(asce)0733-9445(1997)123:7(903).

[12] Cao, V. V. (2025). Effects of CFRP U-Wraps on the Behavior of NSM GFRP Retrofitted Reinforced Concrete Beams. Journal of Composites for Construction, 29(1). doi:10.1061/jccof2.cceng-4884.

[13] Ahmad, H., Hameed, R., Riaz, M. R., & Gillani, A. A. (2018). Strengthening of concrete damaged by mechanical loading and elevated temperature. Advances in Concrete Construction, 6(6), 645–658. doi:10.12989/acc.2018.6.6.645.

[14] Zhao, K., Hu, Z., Wang, B., Wen, Y., Han, J., Wu, Q., & Xu, Y. (2024). Experimental investigation on axial compression behavior of heat-damaged concrete cylinders confined with CFRP sheets. Structures, 70, 107560. doi:10.1016/j.istruc.2024.107560.

[15] Limwibul, V., Jirawattanasomkul, T., Jongvivatsakul, P., Likitlersuang, S., Dai, J. G., & Ueda, T. (2024). Stress-strain behaviour of pre-damaged concrete confined with natural fibre reinforced polymer. Structures, 69, 107434. doi:10.1016/j.istruc.2024.107434.

[16] Saadatmanesh, H., Ehsani, M. R., & Jin, L. (1997). Repair of earthquake-damaged RC columns with FRP wraps. ACI Structural Journal, 94(2), 206–X. doi:10.14359/474.

[17] Lao, X., Han, X., Ji, J., & Chen, B. (2019). The compression behavior of CFRP-repaired damaged square RC columns. Construction and Building Materials, 223, 1154–1166. doi:10.1016/j.conbuildmat.2019.07.182.

[18] Ozcan, O., Binici, B., Canbay, E., & Ozcebe, G. (2010). Repair and strengthening of reinforced concrete columns with CFRPs. Journal of Reinforced Plastics and Composites, 29(22), 3411–3424. doi:10.1177/0731684410376332.

[19] Cao, V. Van, Dinh, L. H., Trinh, L. C., & Vo, H. B. (2023). Behavior of postfire RC columns retrofitted with CFRP wraps under monotonic and cyclic axial loadings: Experiments and theoretical analyses. Journal of Building Engineering, 72(106657). doi:10.1016/j.jobe.2023.106657.

[20] Nguyen, T. H., Nguyen, V. T., Pham, X. D., Nguyen, M. H., & Le, P. L. (2024). Experimental Study on the Strengthening Effect of CFRP Sheets on Corrosion-Damaged, Eccentrically Loaded Reinforced Concrete Columns. International Journal of Civil Engineering, 22(4), 535–547. doi:10.1007/s40999-023-00911-8.

[21] Mostofinejad, D., Abdoli, M., Savoj, M., & Hajrasouliha, M. (2024). Hybrid rehabilitation of 3D RC beam-column joints using UHP-HFRC and FRP wrapping: Experimental evaluation and theoretical analysis. Journal of Building Engineering, 97, 110758. doi:10.1016/j.jobe.2024.110758.

[22] Balsamo, A., Colombo, A., Manfredi, G., Negro, P., & Prota, A. (2005). Seismic behavior of a full-scale RC frame repaired using CFRP laminates. Engineering Structures, 27(5), 769–780. doi:10.1016/j.engstruct.2005.01.002.

[23] Bagheri, M., Chahkandi, A., & Jahangir, H. (2019). Seismic Reliability Analysis of RC Frames Rehabilitated by Glass Fiber-Reinforced Polymers. International Journal of Civil Engineering, 17(11), 1785–1797. doi:10.1007/s40999-019-00438-x.

[24] Van Cao, V., & Quoc Nguyen, T. (2019). Effects of CFRP/GFRP flexural retrofitting on reducing seismic damage of reinforced concrete frames: a comparative study. Asian Journal of Civil Engineering, 20(8), 1071–1087. doi:10.1007/s42107-019-00173-7.

[25] Lam, L., & Teng, J. G. (2003). Design-oriented stress-strain model for FRP-confined concrete. Construction and Building Materials, 17(6–7), 471–489. doi:10.1016/S0950-0618(03)00045-X.

[26] Lam, L., & Teng, J. G. (2003). Design-oriented stress-strain model for FRP-confined concrete in rectangular columns. Journal of Reinforced Plastics and Composites, 22(13), 1149–1186. doi:10.1177/0731684403035429.

[27] Harajli, M. H., Hantouche, E., & Soudki, K. (2006). Stress-strain model for fiber-reinforced polymer jacketed concrete columns. ACI Structural Journal, 103(5), 672–682. doi:10.14359/16919.

[28] Wu, G., Wu, Z. S., & Lü, Z. T. (2007). Design-oriented stress-strain model for concrete prisms confined with FRP composites. Construction and Building Materials, 21(5), 1107–1121. doi:10.1016/j.conbuildmat.2005.12.014.

[29] Wei, Y. Y., & Wu, Y. F. (2012). Unified stress-strain model of concrete for FRP-confined columns. Construction and Building Materials, 26(1), 381–392. doi:10.1016/j.conbuildmat.2011.06.037.

[30] Van Cao, V., & Pham, S. Q. (2019). Comparison of CFRP and GFRP Wraps on Reducing Seismic Damage of Deficient Reinforced Concrete Structures. International Journal of Civil Engineering, 17(11), 1667–1681. doi:10.1007/s40999-019-00429-y.

[31] Harajli, M. H., & Rteil, A. A. (2004). Effect of Confinement Using Fiber-Reinforced Polymer or Fiber-Reinforced Concrete on Seismic Performance of Gravity Load-Designed Columns. ACI Structural Journal, 101(1), 47–56. doi:10.14359/12997.

[32] Sheikh, S. A., & Yau, G. (2002). Seismic behavior of concrete columns confined with steel and fiber-reinforced polymers. ACI Structural Journal, 99(1), 72–80. doi:10.14359/11037.

[33] Rahai, A., & Akbarpour, H. (2014). Experimental investigation on rectangular RC columns strengthened with CFRP composites under axial load and biaxial bending. Composite Structures, 108(1), 538–546. doi:10.1016/j.compstruct.2013.09.015.

[34] Mostofinejad, D., Moshiri, N., & Mortazavi, N. (2015). Effect of corner radius and aspect ratio on compressive behavior of rectangular concrete columns confined with CFRP. Materials and Structures, 48(1–2), 107–122. doi:10.1617/s11527-013-0171-9.

[35] Wang, L. M., & Wu, Y. F. (2008). Effect of corner radius on the performance of CFRP-confined square concrete columns: Test. Engineering Structures, 30(2), 493–505. doi:10.1016/j.engstruct.2007.04.016.

[36] Yang, X., Wei, J., Nanni, A., & Dharani, L. R. (2004). Shape Effect on the Performance of Carbon Fiber Reinforced Polymer Wraps. Journal of Composites for Construction, 8(5), 444–451. doi:10.1061/(asce)1090-0268(2004)8:5(444).

[37] Zhu, J. Y., Lin, G., Teng, J.-G., Chan, T.-M., Zeng, J.-J., & Li, L.-J. (2020). FRP-Confined Square Concrete Columns with Section Curvilinearization under Axial Compression. Journal of Composites for Construction, 24(2). doi:10.1061/(asce)cc.1943-5614.0000999.

[38] Zeng, J. J., Teng, J. G., Lin, G., & Li, L. J. (2021). Large-Scale FRP-Confined Rectangular RC Columns with Section Curvilinearization under Axial Compression. Journal of Composites for Construction, 25(3), 04021020. doi:10.1061/(asce)cc.1943-5614.0001129.

[39] He, C., & Zeng, J. J. (2022). Fiber-Reinforced Polymer-Confined Non-Circular Columns with Shape Modification: A Comprehensive Review. Polymers, 14(3), 564. doi:10.3390/polym14030564.

[40] Pantelides, C., & Yan, Z. (2006). FRP Jacketed and Shape-Modified Compression Members: I–Experimental Behavior. Structural Journal, 103(6), 226-234. doi:10.14359/18243.

[41] Pantelides, C. P., & Yan, Z. (2007). Confinement model of concrete with externally bonded FRP jackets or posttensioned FRP shells. Journal of Structural Engineering, 133(9), 1288-1296. doi:10.1061/(ASCE)0733-9445(2007)133:9(1288).

[42] Yan, Z., & Pantelides, C. P. (2011). Concrete column shape modification with FRP shells and expansive cement concrete. Construction and Building Materials, 25(1), 396–405. doi:10.1016/j.conbuildmat.2010.06.013.

[43] Pham, T. M., Doan, L. V., & Hadi, M. N. S. (2013). Strengthening square reinforced concrete columns by circularisation and FRP confinement. Construction and Building Materials, 49, 490–499. doi:10.1016/j.conbuildmat.2013.08.082.

[44] Hadi, M. N. S., Pham, T. M., & Lei, X. (2013). New Method of Strengthening Reinforced Concrete Square Columns by Circularizing and Wrapping with Fiber-Reinforced Polymer or Steel Straps. Journal of Composites for Construction, 17(2), 229–238. doi:10.1061/(asce)cc.1943-5614.0000335.

[45] Zeng, J.-J., Guo, Y.-C., Gao, W.-Y., Li, J.-Z., & Xie, J.-H. (2017). Behavior of partially and fully FRP-confined circularized square columns under axial compression. Construction and Building Materials, 152, 319–332. doi:10.1016/j.conbuildmat.2017.06.152.

[46] Hadi, M. N. S., Jameel, M. T., & Sheikh, M. N. (2017). Behavior of Circularized Hollow RC Columns under Different Loading Conditions. Journal of Composites for Construction, 21(5), 04017025. doi:10.1061/(asce)cc.1943-5614.0000808.

[47] Jameel, M. T., Sheikh, M. N., & Hadi, M. N. S. (2017). Behaviour of circularized and FRP wrapped hollow concrete specimens under axial compressive load. Composite Structures, 171, 538–548. doi:10.1016/j.compstruct.2017.03.056.

[48] Mai, A. D., Sheikh, M. N., & Hadi, M. N. S. (2019). Performance evaluation of intermittently CFRP wrapped square and circularised square reinforced concrete columns under different loading conditions. Structure and Infrastructure Engineering, 15(5), 696–710. doi:10.1080/15732479.2019.1572201.

[49] Al-Tameemi, H., & Akın, E. (2022). Improving the efficiency of FRP-Confined square concrete column by rounding the sharp edges and circularizing the flat sides. Structures, 45, 1762–1773. doi:10.1016/j.istruc.2022.10.014.

[50] TCVN 7570:2006. (2006). Aggregates for concrete and mortar–Specifications. Vietnam National Standard, Hanoi, Vietnam. (In Vietnamese).

[51] Rocca, S., Galati, N., & Nanni, A. (2009). Interaction diagram methodology for design of FRP-confined reinforced concrete columns. Construction and Building Materials, 23(4), 1508–1520. doi:10.1016/j.conbuildmat.2008.06.010.

[52] ACI 440.2R-08. (2008). Guide for the Design and Construction of Externally Bonded FRP Systems for Strengthening Concrete Structures. American Concrete Institute (ACI), Michigan, United States.

[53] Park, R., & Paulay, T. (1975). Reinforced Concrete Structures. John Wiley & Sons, Hoboken, United States. doi:10.1002/9780470172834.

[54] Realfonzo, R., & Napoli, A. (2013). Confining concrete members with FRP systems: Predictive vs design strain models. Composite Structures, 104, 304–319. doi:10.1016/j.compstruct.2013.04.031.

[55] Baji, H. (2017). Calibration of the FRP Resistance Reduction Factor for FRP-Confined Reinforced Concrete Building Columns. Journal of Composites for Construction, 21(3), 04016107. doi:10.1061/(asce)cc.1943-5614.0000769.

[56] Baji, H., Ronagh, H. R., & Li, C. Q. (2016). Probabilistic Design Models for Ultimate Strength and Strain of FRP-Confined Concrete. Journal of Composites for Construction, 20(6), 04016051. doi:10.1061/(asce)cc.1943-5614.0000704.